Aging Cell (2013) **12**, pp398–409 Doi: 10.1111/acel.12063

WormFarm: a quantitative control and measurement device toward automated *Caenorhabditis elegans* aging analysis

Bo Xian,[1,3]* Jie Shen,[2]* Weiyang Chen,[1]* Na Sun,[1,3] Nan Qiao,[1,3] Dongqing Jiang,[2] Tao Yu,[1] Yongfan Men,[2] Zhijun Han,[1] Yuhong Pang,[2] Matt Kaeberlein,[4] Yanyi Huang[2] and Jing-Dong J. Han[1]

[1]CAS Key Laboratory for Computational Biology, CAS-Max Planck Partner Institute for Computational Biology, Shanghai Institutes for Biological Sciences, Chinese Academy of Sciences, 320 Yueyang Road, Shanghai 200031, China
[2]College of Engineering and Biodynamic Optical Imaging Center (BIOPIC), Peking University, Beijing 100871, China
[3]Center for Molecular Systems Biology, Institute of Genetics and Developmental Biology, Chinese Academy of Sciences, Lincui East Road, Beijing 100101, China
[4]Department of Pathology, University of Washington, Seattle, WA 98195, USA

Summary

***Caenorhabditis elegans* is a leading model organism for studying the basic mechanisms of aging. Progress has been limited, however, by the lack of an automated system for quantitative analysis of longevity and mean lifespan. To address this barrier, we developed 'WormFarm', an integrated microfluidic device for culturing nematodes. Cohorts of 30–50 animals are maintained throughout their lifespan in each of eight separate chambers on a single WormFarm polydimethylsiloxane chip. Design features allow for automated removal of progeny and efficient control of environmental conditions. In addition, we have developed computational algorithms for automated analysis of video footage to quantitate survival and other phenotypes, such as body size and motility. As proof-of-principle, we show here that WormFarm successfully recapitulates survival data obtained from a standard plate-based assay for both RNAi-mediated and dietary-induced changes in lifespan. Further, using a fluorescent reporter in conjunction with WormFarm, we report an age-associated decrease in fluorescent intensity of GFP in transgenic worms expressing GFP tagged with a mitochondrial import signal under the control of the *myo-3* promoter. This marker may therefore serve as a useful biomarker of biological age and aging rate.**

Key words: aging; automatic; *C. elegans*; microfluidics; phenotype; quantitative analysis.

Correspondence
Jing-Dong J. Han, CAS Key Laboratory for Computational Biology, CAS-Max Planck Partner Institute for Computational Biology, Shanghai Institutes for Biological Sciences, Chinese Academy of Sciences, 320 Yueyang Road, Shanghai, 200031, China. Tel.: 86 21 54920458; fax: 86 21 54920504; e-mail: jdhan@picb.ac.cn
or
Yanyi Huang, College of Engineering, and Biodynamic Optical Imaging Center (BIOPIC), Peking University, Beijing, 100871, China. Tel.: 86 10 62758323; fax: 86 10 62758323; e-mail: yanyi@pku.edu.cn

*These authors contributed equally to this work.

Accepted for publication *12 February 2013*

Introduction

The nematode *Caenorhabditis elegans* has been a primary model organism for studying basic mechanisms of aging. Powerful *C. elegans* genetics have enabled discovery of hundreds of lifespan extending mutations and delineated novel longevity pathways. Moreover, phenotypic assays have been developed that allow quantitative assessment of mean lifespan (Huang *et al.*, 2004; Gerstbrein *et al.*, 2005; Leiser *et al.*, 2011). Importantly, several of the aging-related factors uncovered from studies in *C. elegans*, such as the insulin/IGF-1 signaling (IIS) pathway and the target of rapamycin (TOR) kinase, are now known to similarly modulate longevity and aging in mammals (Kenyon, 2010).

As a widely used model system for aging-related studies, maximal lifespan and mean lifespan analyses in *C. elegans* are essential experiments in many laboratories. However, the standard assays are tedious, time-consuming, and susceptible to human bias and technical variations. For example, to measure lifespan, researchers typically maintain animals on Nematode Growth Medium (NGM) agar plates with a lawn of *Escherichia coli* OP50 as the food source (Brenner, 1974; Sutphin & Kaeberlein, 2009). Adult animals must be transferred to fresh plates every few days to prevent depletion of the food source or contamination with progeny. The amount of manual labor required to perform lifespan analysis in *C. elegans* can be reduced somewhat using the drug 2′-deoxy-5-fluorouridine (Floxuridine, FUdR) to prevent hatching of eggs (Mitchell *et al.*, 1979; Gandhi *et al.*, 1980); however, animals must still be periodically transferred to fresh NGM plates to avoid contamination and maintain stable RNAi efficacy and are manually assessed for viability every 2–4 days.

In addition to the large amount of effort required to perform longevity studies in *C. elegans*, a variety of environmental factors limit the quantitative resolution and reproducibility of these assays. For example, contamination of the NGM agar with bacteria and/or fungi, variation in temperature and moisture, and loss of animals due to foraging are all likely to contribute to variations between experiments within the same laboratory and among different laboratories. Addition of FUdR may also influence longevity under some conditions, such as its reported effect of enhancing the lifespan of *tub-1* mutants (Aitlhadj & Sturzenbaum, 2010), masking lifespan extension caused by *ash-2(RNAi)* (Greer *et al.*, 2010), and affecting the identification of metabolic responses to *daf-2* status (Davies *et al.*, 2012).

Lifespan assays can also be performed on solid NGM overlaid with a liquid layer (Bishop & Guarente, 2007). However, these types of protocols are less commonly employed, because several potential problems have thus far limited the utility and generality of liquid-based longevity protocols. These include the difficulty in separating adult hermaphrodites from their progeny (without FUdR) and the need to frequently transfer the worms to fresh medium over the course of the lifespan. Relative to the number of studies performed

on solid media, there are far fewer reports of quantitative lifespan assays performed in liquid culture, and these have generally been low throughput (Hulme *et al.*, 2010).

An automated method to quantitatively measure survival and age-related phenotypes would represent a major breakthrough in methodology and benefit the field substantially. Microfluidics-based systems for culturing nematodes offer an attractive approach toward developing such a system. For example, Hulme *et al.* have recently proposed a microfluidic method to make lifelong observations of a few animals (Hulme *et al.*, 2010). To date, however, no practical microfluidic device for monitoring and collecting lifelong age-related data on a large population of animals has been described. Here, we present such a system. WormFarm is an integrated microfluidic platform to maintain groups of nematodes during adulthood, along with a set of algorithms to quantitate survival and age-related phenotypes from images and videos. As proof-of-principle, we performed survival analysis of wild-type (N2) animals subjected to three RNAi knockdowns and glucose treatment previously reported to influence longevity. We also carried out real-time fluorescence imaging of intestinal auto-fluorescence and muscle-expressed mitochondria-targeted GFP (*Pmyo-3::mito::GFP*) in animals as they aged. This novel approach allowed us to identify a previously undetected reduction in *Pmyo-3::mito::GFP* fluorescence with age. This trend was observed in all RNAi and control strains and scaled to lifespan, suggesting that this marker may serve as a useful biomarker of biological age or rate of aging.

Results

The design of WormFarm platform

The WormFarm platform is composed of 3 modules: food/medium loading module, WormFarm chip, and image acquisition module. The food suspension (*E. coli* OP50) is stored inside the 15-ml conical bottom culture tubes with tubing connected to the microfluidic chip. Compressed air is used to drive the food into the culture chambers on-chip (Fig. 1).

The WormFarm chip is a multilayer polydimethylsiloxane (PDMS) microfluidic device with monolithic integrated controllable valves (Fig. 1). The eight chambers (3×10 mm^2 each) per chip are completely separated from each other to prevent cross-contamination and are optimized to culture ~ 40 animals per chamber (Fig. 1). The upper boundaries of the chambers are arc-shaped to prevent liquid and small larvae from being trapped in corners. The typical thickness of an N2 adult worm is ~ 90 μm; thus, the height of the chamber is 100 μm to allow the animals to move freely. At the downstream boundary of the chamber, there is a channel-comb, composed of a row of small channels, each of which is 20 μm wide and 10 μm high. These channels function like a sieve, preventing passage of adult animals but filtering L1 or L2 larvae from the chamber. To prevent blocking of the sieve channels by adult animals, extra sieve channels were also placed on the sides of the chamber. Bypass channels are present in each culture chamber to remove air bubbles when loading samples and food/medium. All channels are controlled by monolithic pneumatic valves (Unger *et al.*, 2000; Thorsen *et al.*, 2002) (Fig. 1). Waste is discharged from the outlets of the chambers via tubing connections. These exits may also be used to collect the larvae if desired, for example, to examine phenotypic changes in progeny as a function of parents' age. If recovery of adults is desired, the chambers can be reversely flushed with culture medium to remove the animals from inlets. PDMS is intrinsically transparent, allowing visualization of the animals inside the culture chambers by microscopy using standard equipment.

Loading and operating the device

Each PDMS chamber is designed to be loaded with approximately 40 adult nematodes (Fig. S1, Video S1, S2). Prior to loading the

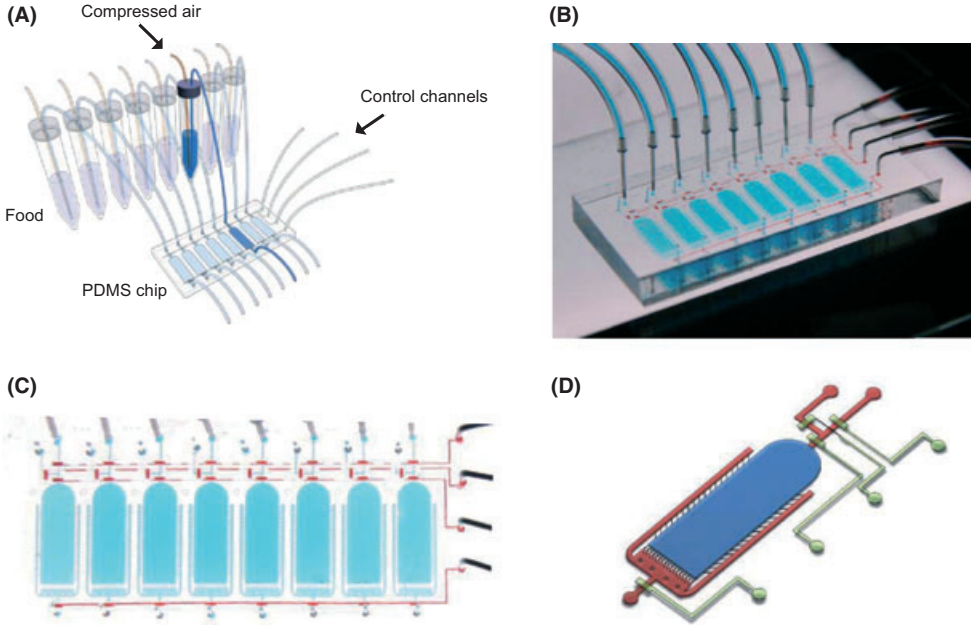

Fig. 1 Design of the WormFarm system. (a) Schematic of the WormFarm platform. (B) A photograph of the WormFarm chip. A 25×55 mm^2 chip is mounted at the center of a 70×100 mm^2 glass slide. (C) Each chip contains eight separated chambers, which can be controlled by the pneumatic valves simultaneously. (D) 3D schematic of a single WormFarm chamber, with narrow channels at side and bottom edge to filter out the worm progeny by size.

animals, each chamber is incubated with 0.2% Pluronic solution [0.2% w/v cell culture grade Pluronic F127 (Sigma, St. Louis, MO, USA)] for 30 min followed by rinsing with S-Medium. Pluronic solution is a kind of surface-activating agent, which prevents free bacteria from depositing on the surface of the PDMS. Following the rinse, 200 μL of a suspension containing synchronized young adult animals in S-Medium (~ 200 nematodes mL^{-1}) is then loaded in each chamber and the valves are closed. Food supply tubes are then connected to provide a flow of bacterial food to each chamber. Here, we used the bacterial concentrations of 10^9 cell mL^{-1} in S-Medium for liquid culture (Bishop & Guarente, 2007) to ensure sufficient food for the worms. The valves for worm loading are closed after loading. Flow rates and number of animals are visually optimized to the minimal flow that can disperse the worms at a comfortable level and wash out the progenies. As a result of such testing, the period of the flow cycle of the food/medium supply is set to 2.5 min, and the flow/stop ratio of each cycle was set to be 0.25 (0.5 min influx with 2 min in between) through the control of the valves. Under these conditions, all progeny are washed out of the chambers through the outlets as L1 or L2 larvae (Video S3). This eliminates the need for adding FUdR to the medium.

Validation of WormFarm for nematode culture

A critical first test of WormFarm is to verify that the health of animals maintained in the microfluidic chamber is similar to animals aged under conventional agar-plate-based conditions. We therefore performed parallel studies of animals maintained either in WormFarm or on NGM plates from adult day 2 to adult day 8 and quantified the size of worms under both conditions. As the densities and environments of worms are quite different in those two conditions, the worms in chips were generally smaller than those on plates. However, the inter-strain differences largely followed the same trend, and the worms' average body size increased from day 2 to day 5 in most of the strains under both conditions (Fig. S2). These indicate that the worms in WormFarm grew as well as those on plates.

The automation of progeny separation, continuous food supply, and waste control are obvious advantages of WormFarm over the conventional approaches. In this study, we typically carried out experiments with 2–4 WormFarm chips simultaneously. Using a 2-chip experiment as an example, once the chambers are loaded, lifespan is determined for ~ 640 animals without requiring additional manual intervention. For comparison, the same experiment performed using the standard plate-based assay would require manual transfers of ~ 640 animals at least 3–5 times and manual determination of viability for each animal by prodding every 2–3 days. Thus, WormFarm provides a much simpler, less invasive, and more efficient way to perform these types of experiments with the added advantage of providing dynamic control of the culture conditions.

Validation of WormFarm for RNAi studies

RNAi has proven to be a particularly powerful technique to probe genetic regulation of aging in *C. elegans*. To determine whether WormFarm can be used to quantitate lifespan in conjunction with RNAi knockdown, N2 animals were aged in WormFarm and fed with HT115 bacteria containing either an empty-vector control plasmid or sequence-confirmed RNAi plasmids targeting *sptf-3*, *Y82E9BR.3*, or *age-1* from a genome-wide RNAi library, the Ahringer library (Fraser *et al.*, 2000; Timmons *et al.*, 2001). Survival was determined by video microscopy of each WormFarm chamber. RNAi knockdown of *sptf-3* is reported to result in shorter lifespan (Xue *et al.*, 2007), while knockdown of an ATP synthesis gene such as *Y82E9BR.3,* reduces body size and extends lifespan (Lee *et al.*, 2003). In both cases, the lifespans obtained from animals aged in WormFarm showed the expected trends and matched the survival of animals aged on NGM plates (Fig. 2, Fig. S3, Table 1). In the case of *Y82E9BR.3(RNAi)*, the body size reduction and the developmental delay were clearly observed in animals cultured in WormFarm, while *sptf-3(RNAi)* resulted in a shorter lifespan than the control group, as previously described (Xue *et al.*, 2007) (Fig. 2, Video S3).

The IIS pathway is the best-characterized longevity pathway in *C. elegans*. Reduced signaling through this pathway leads to the activation of FOXO-family transcription factor DAF-16 (Lin *et al.*, 1997; Ogg *et al.*, 1997) and results in robust lifespan extension. Reduction-of-function mutations or RNAi knockdown of several components of this pathway, including the genes encoding the insulin-like receptor *daf-2* or the PI3-kinase *age-1*, has been reported by many laboratories to enhance longevity (Johnson, 1990; Morris *et al.*, 1996; Kenyon, 2005). As further validation of WormFarm, we examined the effect of RNAi knockdown of *age-1* on animals maintained in WormFarm. As expected, lifespan was significantly extended relative to control animals.

In all of these experiments, RNAi knockdown was carried out by simply replacing the OP50 suspension with the appropriate RNAi bacterial strain grown under inducing conditions. Even though the repeats of RNAi lifespan assays were derived from independent chips, both the survival rates on each day (Fig. 2, Fig. S3c) and the overall mean lifespan differences (Table S1) showed good repeatability of WormFarm.

Viability of individual animals in WormFarm is determined from videos that are acquired daily using an algorithm we developed (see below). This is a substantial improvement in efficiency compared with the manual determination of viability by gently tapping each animal on the head to tell whether it is alive or dead. WormFarm allows for automatic collection and in-line analysis of the quantitative imaging data, which is acquired as frequently as required.

Effect of glucose supplementation on lifespan using WormFarm

In addition to the reduced time, effort, and resources required to perform aging-related analyses using WormFarm, the ease with which the effects of different medium compositions can be examined is a major advantage of this system. Changes in medium compositions could involve dietary interventions, such as dietary restriction, or pharmacological interventions for drug screening and/or toxicology studies.

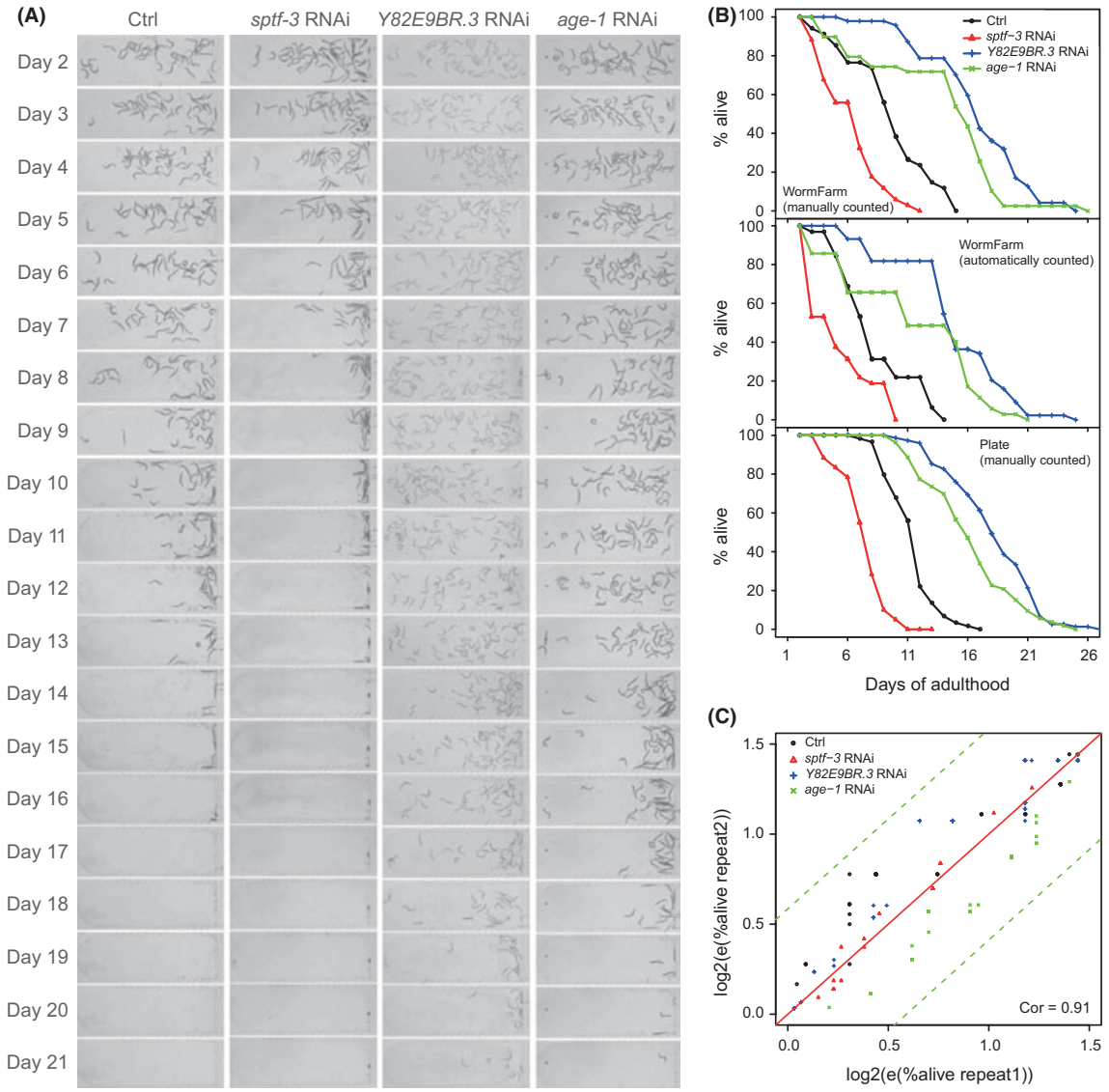

Fig. 2 Lifespan assays for worms fed RNAi bacteria in WormFarm. (A) Photographs of worms living in WormFarm PDMS chambers under different RNAi conditions. (B) Survival rate curves of worms in PDMS chambers upon different RNAi conditions when live worms were determined manually by watching movies (upper panel) or by computational program analyzing the movies (middle panel), and the survival rate curves of worms under different RNAi treatments on NGM plates when live worms were determined by conventional method (lower panel). The day of egg-laying was defined as day 0 in all the experiments in this study. Lifespan of adulthood were obtained at 25 °C. (C) Scatter plots showing the repeatability of each group of two biological replicates in different chambers on different chips. Survival rates of two different repeats are plotted against each other across the worm adult lifespan. The *x*- and *y*-axes indicate the survival rates of repeat 1 and repeat 2 on the indicated day of adult life, respectively. Pearson correlation coefficient ('Cor') between the repeats for all four groups is shown at the bottom of the panel. Raw data are available in Table S4 (Supporting Information).

One dietary intervention that has been reported to shorten *C. elegans* lifespan is addition of glucose to the diet (Schulz *et al.*, 2007; Lee *et al.*, 2009; Schlotterer *et al.*, 2009). Consistent with this, we observed that supplementation with either 2 or 4% glucose shortened the lifespan of animals aged in WormFarm or on NGM agar plates (Fig. 3, Fig. S4a). These experiments demonstrate that WormFarm is able to detect subtle effects on longevity, such as the ~ 15% average lifespan reductions induced by 2 or 4% glucose compared with control (Table 2). Furthermore, these experiments again demonstrate good repeatability of the survival rates of worms on each day (Fig. 3, Fig. S4c) of the WormFarm system, which is similar to that obtained by routine on-plate experiments (Fig. S4b), and also good repeatability of the overall mean lifespan differences (Table S2) among independent devices. Overall, subtle environmental differences, such as the concentration and the form of food, and differences in humidity and temperature can be precisely controlled in WormFarm, resulting in very good repeatability (Fig. 2, 3, Fig. S3c, S4c, Table S1 and S2).

Quantitative phenotypic analysis in WormFarm assisted by automatic imaging analysis

The tremendous amount of data (~ 100 GB of images and video per experiment), automatically collected by WormFarm, provides both

Table 1 Significance of deviation of a survival rate curve from the control curve in RNAi experiments

Group	RNAi	Mean lifespan (day)	Max lifespan (day)	Standard deviation	Mean lifespan change (%)	*n*	*P*-value
WormFarm manually counted	ctrl	8.676470588	14	3.435294423		34	
	sptf-3	5.382352941	11	2.474288461	−37.97	34	6.39E-06
	age1	13	25	5.472418882	49.83	39	1.84E-07
	Y82E9BR.3	15.93617021	24	4.088181563	83.67	47	9.66E-15
WormFarm automatically counted	ctrl	7.34375	13	3.064988291		32	
	sptf-3	4.34375	9	2.719219231	−40.85	32	0.000687
	age1	10.6	20	5.595165981	44.34	35	0.000127
	Y82E9BR.3	13.93181818	24	4.505282312	89.71	44	1.33E-12
NGM plate	ctrl	10.45762712	16	1.985482083		59	
	sptf-3	6.483333333	10	1.836463686	−38.00	60	< 2.2E-16
	age1	15.22641509	24	3.739814421	45.60	53	5.7E-14
	Y82E9BR.3	17.24	26	3.552083515	64.86	75	< 2.2E-16

an opportunity and a challenge for quantitative analysis. To maximize the information obtained from each experiment, we developed computational image analysis algorithms (Experimental procedures and Note S1) to automatically analyze the video footage and quantitate survival rate (live or dead worms) and other phenotypes including worm size, length, width, shape, and content density. (Fig. 4, Video S4, 5). These algorithms generated similar survival curves to those obtained by manual analysis and correctly recapitulated the observed differences in lifespan for all of the experiments (Table S1, S2). In addition, they provide quantitative analysis of the body size and motility parameters with age in real time. Using these algorithms, we found that the long-lived *age-1(RNAi)* and *Y82E9BR.3(RNAi)* animals were significantly thinner (Student's *t*-test $P = 2.2e\text{-}16$ and 3.39e-12, respectively. Fig. 4) and more active than the control group (Fig. 4, $P = 3.43e\text{-}9$ and 1.75e-6, respectively). In contrast, the short-lived *sptf-3(RNAi)* animals had larger body width (Fig. 4, $P = 4.83e\text{-}2$). The motility of *sptf-3(RNAi)* animals was significantly less than the other three groups ($P = 3.35e\text{-}5$, 2.2e-16, and 1.05E-12 vs. control, *age-1,* and *Y82E9BR.3*, respectively, Fig. 4 and Table S3). In fact, if the anatomical features of the single worms in each picture were classified using principal component analysis (PCA), the first and third principal (PC1 and PC3) components jointly separated the *Y82E9BR.3(RNAi)* strain from the other three strains, and the young and old worm in each strain were distributed diagonally between PC1 and PC3 (Fig. 4). The major contributing features to PC1 are size (0.44) and mean gray density (−0.43), while shape and gray density distribution contribute the most to PC3 (−0.67 and −0.52, respectively), suggesting these features are most associated with age.

These phenotypic data demonstrate yet another significant advantage of WormFarm: multiple aging-related phenotypes can be simultaneously, automatically, and quantitatively analyzed.

Fluorescence-based phenotypic analysis in WormFarm assisted by automatic imaging analysis

In addition to light microscopy, the WormFarm PDMS chambers are also compatible with fluorescence microscopy, and a variety of transgenic fluorescent protein reporters have been constructed for use in *C. elegans*. Of particular interest with respect to age-related changes are markers of mitochondrial biogenesis and function. Enhanced mitochondrial biogenesis is associated with improved mean lifespan in mammals, and mitochondrial gene expression has been shown to decrease with age in many different organisms and tissues (McCarroll *et al.*, 2004; Zahn *et al.*, 2007). For example, we have previously reported that a gene expression module enriched for genes encoding mitochondrial enzymes showed a linear decline with age in adult *Drosophila melanogaster* (Xue *et al.*, 2007).

To examine whether we can detect fluorescence changes *in vivo* with age in live *C. elegans*, we used WormFarm to examine the age-dependent changes in animals expressing a mitochondrial-targeted GFP in muscle cells (*Pmyo-3::mito::GFP*). Consistent with age-dependent oxidative phosphorylation gene expression decline, we observed a continuous decline in fluorescent intensity of GFP with age in worms grown in WormFarm. This decline was very rapid during early adulthood (day 2–7) and slowed down afterward (Fig. 4). RNAi knockdown of *sptf-3*, which shortened lifespan, accelerated the age-dependent decline in GFP fluorescence intensity, while RNAi knockdown of *Y82E9BR.3*, which increased lifespan, delayed the decline (Fig. 4, Fig. S5a). These data suggest that fluorescence intensity of this GFP reporter may serve as a biomarker of biological age and that the rate of the decline may serve as an estimate of aging rate.

Other well-known age-related markers, such as increased intestinal autofluorescence of *C. elegans* during aging (Klass, 1977; Davis *et al.*, 1982; Joeng *et al.*, 2004; Pincus & Slack, 2010), can also be precisely and easily quantified with WormFarm (Fig. 4).

Oxidative stress tolerance assay in WormFarm

In addition to analyzing phenotypes throughout the lifespan of worms, other aging-related parameters can also be quantitatively measured with WormFarm. For example, it is often useful to measure resistance to different forms of stress in addition to lifespan when studying factors that influence longevity. Oxidative stress in particular is linked to aging and lifespan (Finkel & Holbrook, 2000). Using WormFarm, we were able to quantitate increased tolerance to the superoxide generating compound paraquat upon RNAi knockdown of *daf-2*, as well as the greater sensitivity of animals subjected to *daf-16* RNAi (Fig. S6), with differences in survival similar to those

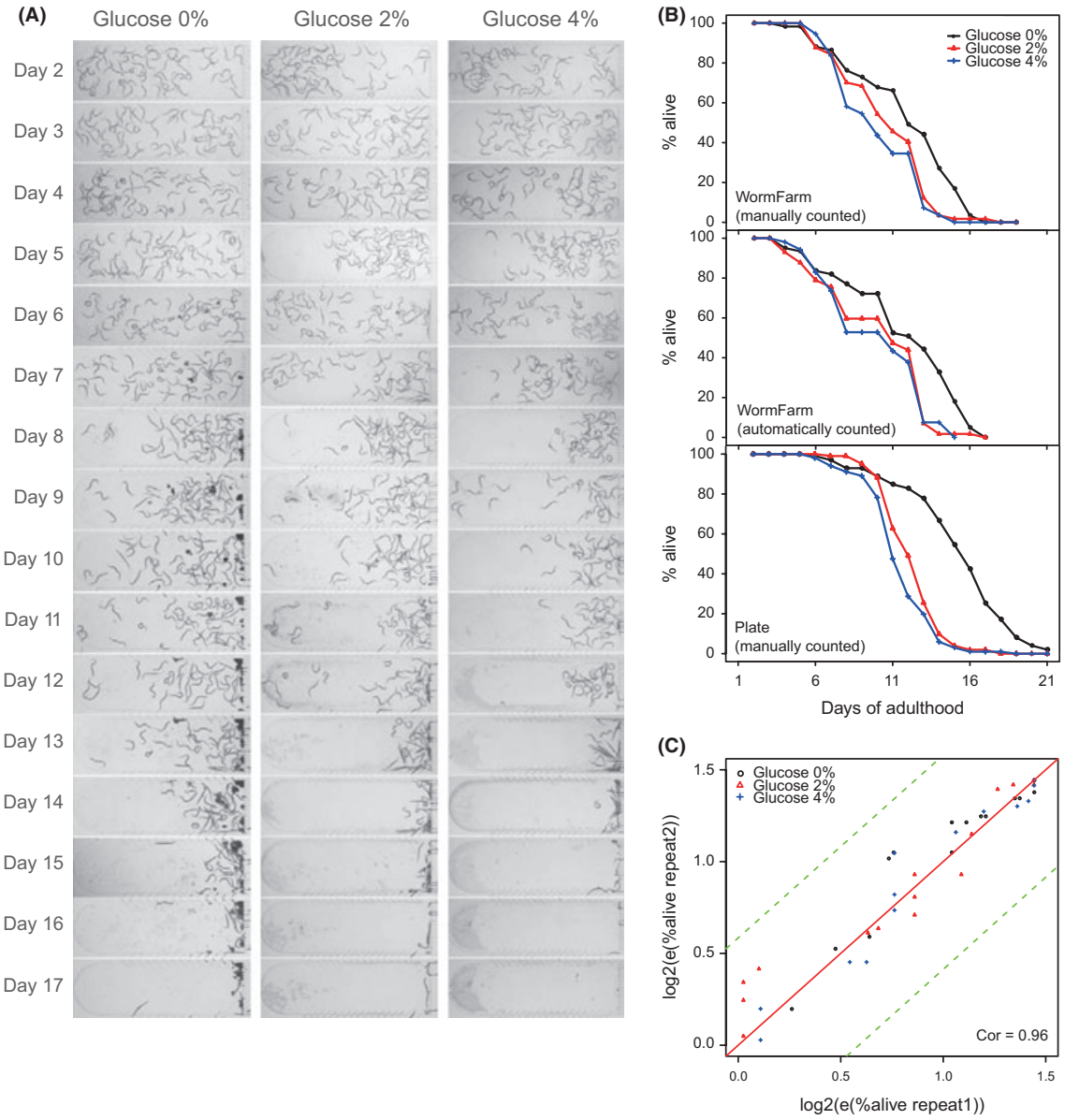

Fig. 3 Lifespan assays for worms in glucose medium. (A) Photographs of worms living in WormFarm PDMS chambers. (B) Survival rate curves of worms in PDMS chambers under different concentrations of glucose when live worms were determined manually by watching movies (upper panel) or by computational program analyzing the movies (middle panel), and the survival rate curves of worms under different concentrations of glucose on NGM plates when live worms were determined by conventional method (lower panel). Lifespan of adulthood was obtained at 25 °C. Live bacteria were fed to the worms according to a previous study (Lee *et al.*, 2009). (C) Scatter plots showing the repeatability of each group of two biological replicates in different chambers on different chips. Survival rates of two different repeats against each other across the worm adult lifespan. The *x*- and *y*-axis indicate the survival rates of repeat 1 and repeat 2 on the indicated day of adult life, respectively. Pearson correlation coefficient ('Cor') between the repeats for all three groups is shown at the bottom of the panel. Raw data are available in Table S4 (Supporting Information).

previously reported (Martin *et al.*, 1996; Finkel & Holbrook, 2000). Like many chemicals, paraquat is an expensive reagent. The drastically reduced volumes required for these types of assays in WormFarm reduces the amount of drug required to ~ 1/100 of what is normally consumed in a multiwell plate assay system.

Discussion

As an automated system based on liquid culture in a PDMS chip, WormFarm is a breakthrough for aging-related and survival-based analyses. WormFarm provides a simple, scalable platform for performing high-throughput survival and quantitative fluorescence assays in *C. elegans* at a cost that is substantially reduced relative to the current state-of-the art methods used in the field.

Although there are small differences in the survival data obtained from WormFarm relative to the standard plate-based method, in every case, the relative effects of different genetic and environmental interventions are quite similar. The differences likely arise from environmental factors, such as liquid versus solid medium culture conditions, worm densities. There are also differences between computer-assisted quantitation and manual visual quantitation that might be mainly due to the different standards used in

Table 2 Significance of deviation of a survival rate curve for glucose diet from the control curve

Group	Growth condition (%)	Mean lifespan (day)	Max lifespan (day)	Standard deviation	Mean lifespan change (%)	*n*	*P*-value
WormFarm	Ctrl	10.94915254	16	3.490991998		59	
manually	Glucose 2	9.719298246	17	2.876967563	−11.23	57	0.004148
counted	Glucose 4	9.145454545	14	2.655659099	−16.47	55	8.99E-05
WormFarm	Ctrl	10.78688525	16	3.834556707		61	
automatically	Glucose 2	9.175438596	16	3.412805753	−14.94	57	0.000912
counted	Glucose 4	9.037735849	14	3.198330479	−16.22	53	0.000436
NGM plate	Ctrl	14.36363636	21	3.456595427		99	
	Glucose 2	11.3627451	17	1.855093153	−20.89	102	< 2.2E-16
	Glucose 4	10.58415842	18	2.164566131	−26.31	101	< 2.2E-16

judging viability of the worms. To achieve automation, the computer program has to use certain thresholds, whereas human eyes and judgment are not subject to the same limitation. However, in terms of counting the relative survival and lifespan differences, the computer algorithm performs as good as manual counting (Fig. S7).

For all of the age-related features except survival, we only used single worms (unclustered worms) in each chamber to ensure the accuracy of the quantitative phenotypes. As analyzing worm clusters is apparently a very complex issue for imaging analysis, even the most recent state-of-art algorithm (Wahlby *et al.*, 2012) cannot practically solve this issue, at least not for images generated from our WormFarm chip. Our worm-counting program can at least partially solve this problem, in that using our algorithm, counting clustered worms consistently improved the accuracy of survival rate calculation than without counting clustered worms (Fig. S7).

Microfluidic devices to automate lifespan assays in yeast have been reported recently (Lee *et al.*, 2012; Xie *et al.*, 2012). Such a device for *C. elegans* has been lacking prior to WormFarm. Pincus *et al.* have developed a practical minimally invasive individual-nematode culture system (MIINCS) (Pincus *et al.*, 2011). Our WormFarm differs from this system in several ways, including the following: (i) in MIINCS, one single egg at the prehatch 'pretzel' stage and a bacterial food source are deposited atop PEG-1000-methacrylate hydrogel pads, whereas WormFarm cultures up to 40 worms for a single chamber in the liquid providing higher throughput; (ii) to prevent progeny contamination, only a sterile strain can be used in MIINCS, whereas WormFarm is suitable for studies of reproductively competent strains without the need for FUdR; (iii) food is never changed in MIINCS, while food (or any other component of the culture medium) in WormFarm can be changed automatically and immediately at any point in the experiment; (iv) culturing the worms on the surface of the plate causes the worms to shrink over time in MIINCS, which does not happen in WormFarm; and (v) MIINCS has only been analyzed by a semi-automated software to quantitate various morphological and image-based features, whereas WormFarm uses a fully automated software to do so.

To further increase the throughput of WormFarm, intelligent sample movement and image acquisition are needed. Possible solutions include translation of the sample stage coordinated with auto-focusing and auto-triggering of camera and light source. Such automation improvements will not only relieve the burden from the researchers, realize even larger-scale experimental design, and save experimental time, but also improve the quality of images, and the precision of data analysis.

In summary, WormFarm is a powerful new resource for aging-related studies in *C. elegans*. For the first time, it is possible to perform fully automated lifespan assays and to obtain quantitative measures of phenotypes such as body size and motility as a function of age without requiring extensive manual manipulation. In addition to reduced manual labor, WormFarm provides many advantages over traditional methods, including (i) alleviating contamination by progeny without use of drugs that inhibit reproduction; (ii) providing improved environmental control; (iii) removing the potential for unintentional human bias by automated acquisition and analysis of images and movies; and (iv) dramatically reducing costs associated with consumption of reagents and chemicals. In this report, we have demonstrated that WormFarm successfully reproduces the expected effects of RNAi knockdown for factors that either shorten or increase lifespan. Further, we have shown that WormFarm can also be used to quantitate changes in the expression of a fluorescence-based reporter during aging and, in the process, discovered a previously unknown inverse relationship between *Pmyo-3::mito::GFP* intensity and age. Indeed, the mito-GFP used in this study appears to provide a useful biomarker of biological age, at least among the interventions tested here.

Experimental procedures

Fabrication of the WormFarm chip

Microfluidic chips were fabricated from polydimethylsiloxane (PDMS) (RTV 615 kit, GE Advanced Materials, Wilton, CT, USA) through multilayer soft lithography (Unger *et al.*, 2000; Thorsen *et al.*, 2002; Wang *et al.*, 2009). The master molds of fluid and control layers were made by photolithography. The silicon wafers were treated with hexamethyldisilazane (Alfa Aesar, Ward Hill, MA, USA) vapor for 3 min at room temperature (25 °C) before coating the photoresist. The hybrid master mold of the fluid layer was fabricated through a multistep photolithography to form the molds with different thickness. The large chambers for worm culture were made of 100-μm-thick negative photoresist (SU-8 2050,

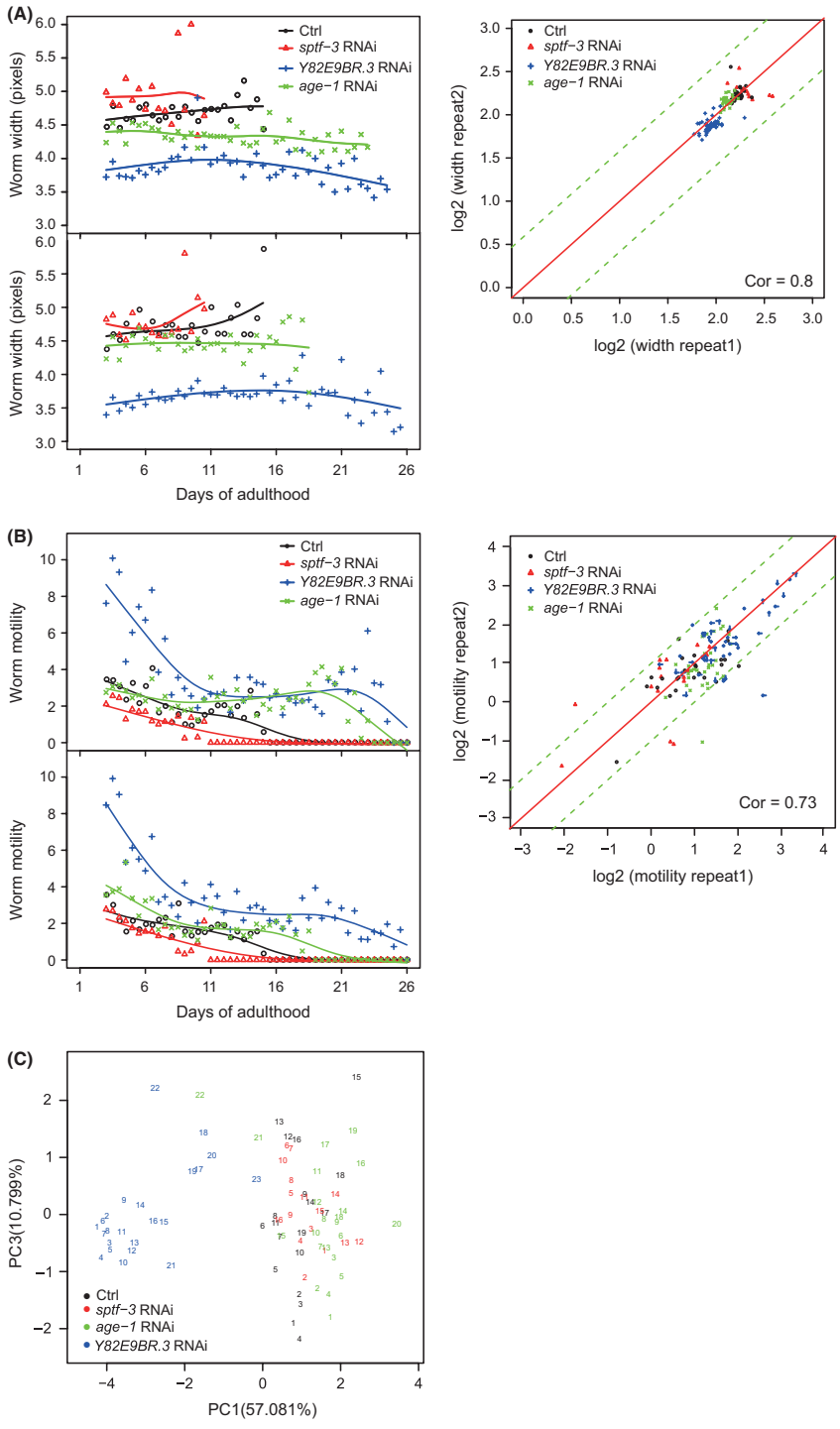

Fig. 4a Aging-related phenotypes quantified by WormFarm. (A, B) The widths and motilities of worms in WormFarm upon RNAi of aging-related genes. The left upper and lower panels display the results from two repeats. Movies taken on each day (Video S4, S5) were analyzed and quantified by our imaging analysis program. The right diagrams show the good repeatability of each group of 2 repeats. Pearson correlation coefficients ('Cor') between the repeats for all four groups are shown at the bottom of the panels. (C) Principal component analysis of various anatomical features of the worm. The worms are arranged according to the first and third principal components of worms' features. These features include shape, area, width, length, average gray value, variance of gray values, and the ratio of pixels brighter than defined threshold. PCA was performed on the average of each feature of all single worms for each age and each RNAi strain. Different RNAi strains are marked by different font colors of the numbers that indicate the age (days) of the worms. (D) *Pmyo-3::mito::GFP* fluorescent intensity over age. Left panels are the fluorescence images on the indicated days of adulthood of the indicated RNAi strains. Right panels show the quantified intensities in the body wall muscles per day per chamber plotted against age. Raw data are available in Table S5 and S6 (Supporting Information). (E) Photographs and quantitation of intestinal auto-fluorescence intensity of N2 worms over age.

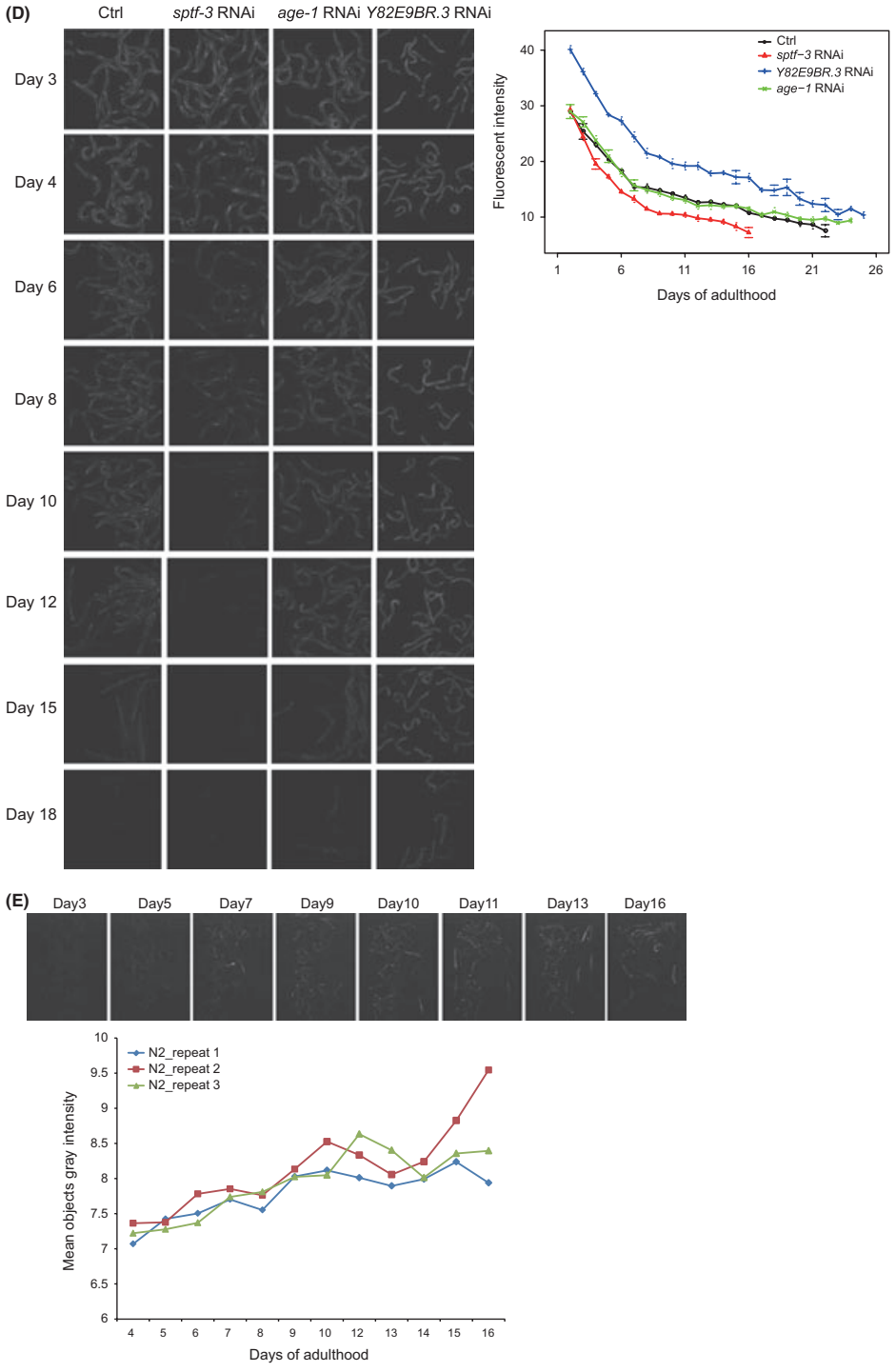

Fig. 4b (Continued).

MicroChem, Newton, MA, USA). The narrow sieve channels were fabricated by spin-coating negative photoresist (SU-8 2010, MicroChem) to a thickness of 10 μm. Other channels that can be controlled by the pneumatic valves were made of 80-μm-thick positive photoresist (AZ 50XT, AZ Electronic Materials). The patterned positive photoresist was re-flowed to obtain a rounded section. The 15-μm-thick mold of the control layer was made of positive photoresist (AZ P4620, AZ Electronic Materials, Branchburg, NJ, USA). The two master molds were treated with trimethylchlorosilane (Sinopharm, Shanghai, China) vapor for 5 min at room temperature before PDMS pouring. 30 g of uncured PDMS mixture (5:1, elastomer-to-cross-linker ratio) was poured onto the master

mold of fluid layer, degassed for 1 h, and then baked at 80 °C for 20 min. The control layer was fabricated by spin-coating uncured PDMS (20:1, elastomer-to-cross-linker ratio) onto the mold at 1200 rpm for 60 s and then was baked at 80 °C for 30 min. After the fluid layer was peeled off from its mold and hole-punched, it was aligned over the control layer and then baked at 80 °C for 45 min. The bonded 2-layer structure was then peeled off from the control mold, hole-punched, and placed on a thin, cured PDMS layer (10:1, elastomer-to-cross-linker ratio) covered glass slide. Finally, the whole chip was incubated at 80 °C for > 6 h to ensure the bonding between layers. We developed a Labview (National Instruments, Austin, TX, USA) program to control the valve actuation, and the fluid flow was driven by compressed air (0.1 MPa).

Worm Synchronization

Four dishes of gravid N2 hermaphrodites were washed off by M9 buffer and then collected and bleached by 5% solution of sodium hypochlorite. After washed by M9 buffer twice, the eggs were suspended in S-medium and allowed to hatch overnight in the absence of food, resulting in starved worms arrested in the L1 stage of development.

Lifespan assays

The day of egg-laying was defined as day 0 for all lifespan tests.

For RNAi-lifespan tests in WormFarm, synchronized L1 worms were distributed to RNAi plates, which had been spread with RNAi bacteria clones, and maintained at 20 °C till adulthood. When reaching adult day 2, worms were washed off the plate and loaded into PDMS chambers of the WormFarm chips and incubated at 25 °C. HT115 bacteria, with RNAi vectors containing different fragments of target genes, were induced by IPTG, suspended in the S-Medium, and passed through the chambers. Fungizone (250 ug L^{-1}) and Amp (100 mg L^{-1}) were added into the S-Medium to prevent the contamination. Bacteria culture was manually changed every day in the food container to maintain fresh food supply.

For the glucose lifespan test in WormFarm, the synchronized L1 worms were cultured on the NGM plates with OP50 bacteria at 20 °C till adulthood. Adult day 2 worms were washed off the plates, loaded into PDMS chambers, and incubated at 25 °C. Fresh live OP50 bacteria stored were suspended in the S-Medium containing different concentrations of glucose (0, 2 and 4%) and passed through the chambers. Fungizone (250 ug L^{-1}) were added into the S-Medium to prevent contamination. Bacteria culture was manually changed every day in the food container to maintain fresh food supply.

Photos and movies of each chamber were taken every 24 h using a CCD camera (DP72, Olympus, Japan) on a zoom stereomicroscope (SMZ1000, Nikon, Japan).

For parallel experiments on NGM agar plates, adult day 2 worms on the RNAi plates were transferred onto new RNAi plates containing 20 μg mL^{-1} FUdR and scored for survival rate every day. Adult day 2 worms for glucose test on NGM plates with OP50 were transferred onto new NGM plates containing 20 μg mL^{-1} FUdR and different concentrations of glucose (0, 2, and 4%) and scored for survival rate every day. Temperature setting was exactly the same as the lifespan test in WormFarm chip: worms grown up at 20 °C and spent adulthood at 25 °C. Worms were transferred to fresh plates every 4 days. Worms that crawled off the plates were excluded from the experiments. All experiments were independently performed at least twice.

Quantitation of the worm phenotypes

All images and videos were collected using a zoom stereomicroscope (Nikon SMZ1000) with a CCD camera (Olympus DP72). The field of view was set to cover one or two chambers for each shot.

To automatically quantitate the survival rate and other phenotypes including worm size, length, and width, we developed a new computational algorithm to analyze the images in three steps.

Step 1: Video preprocessing

We mark the chamber region by first identifying the reference circle in the center of the chip in each frame and then determine the boundaries based on the relative distance to the center of the reference. We then covert the gray-scale images to black and white (BW) images according to Otsu's method (Otsu, 1979). A closed object in the BW image is labeled as a worm-like object (WLO) if its size is $\geq$ 80 pixels.

Step 2: Obtain the maximum area of a single worm (A_{ms})

We define the maximum area in pixels of any single worm (A_{ms}) as 1.5-fold of the median of the WLO's areas on the first video when there is rarely any worm cluster. The A_{ms} is then used to identify single worm and to determine the number of worms in the worm clusters in subsequent videos of older adults, which often contain 2–10 worms per cluster and an average of 35% of the worms clustered in total.

Step 3: Quantitating worm phenotypes

To estimate the number of worms in each WLO, we first label an object as having moved since the last frame (object M) if the nonoverlapping area of the two overlapping WLOs between two frames is > 3% of the union of the two areas. Then, for each M, if its area is $\leq A_{ms}$, the object is labeled as a single worm (SM), and its area, circumference, length, width, mobility (moving area divided by total area) is calculated and recorded (Note S1). And the average size of SMs per chamber, per video is defined as A_{as}. If M's area is $> A_{ms}$, we count the number of single worms as the rounding of the area of M divided by A_{as}. Finally, we calculate the mean value of the worm area/length/width/mobility of all the frames in the video as the average quantified worm phenotypes at a time point (Note S1).

We describe the shape of a worm according to a published method (Stephens *et al.*, 2008). Each single worm was thinned to a backbone (a line of one pixel thick through the center of worm body). We then sliced the backbone to 60 segments to equal arc length and computed each segment's intersection angle with the horizontal axis. To make it independent of coordinate system, all the angles were standardized by subtracting the average of the angles.

A vector of 60 standardized angles of each worm defines the shape of the worm. The average absolute value in each vector was used for PCA. Other features are described in Note S1 (Supporting information), and Image Analysis Tutorials with snapshots are shown in Note S2 (Supporting information).

Mitochondria visualization

Mitochondria were visualized using *Pmyo-3::mito::GFP* construct (Labrousse *et al.*, 1999). We injected the *Pmyo-3::mito::GFP* plasmid into N2 and obtained the stable transgenic line by gamma irradiation.

Real-time *in vivo* fluorescent measurement

For fluorescent intensity of *Pmyo-3::mito::GFP*, N2 worms carrying the *Pmyo-3::mito::GFP* transgene were filmed every day using a fluorescence stereomicroscope with camera (Nikon SMZ1000, Olympus DP72 CCD). The exposure time was set as 50 ms, and sensitivity was ISO1600.

For intestinal auto-fluorescence, N2 worms were filmed every day. The exposure time was set as 200 ms, and sensitivity was ISO1600.

After converting the gray-scale fluorescence images to black and white, we calculated the average signal intensity per pixel per daily image (2× magnification).

For each frame in the fluorescence videos, the pixels that the gray-scale value < 5 were regarded as background, then we could get the objects (each closed area was regarded as an object except those whose area was < 6 pixel); for each objects, the average fluorescent intensity (F) was represented as the average gray-scale values for all the pixels (Note S1). Finally, the F for a video was represented as the average of the F values of the objects from all frames in the video.

Acknowledgments

We thank Bo Zheng (The Chinese University of Hong Kong) for the initial prototype design, Axel Mosig for discussions on image analysis, and Dangsheng Li and Christopher Green for critical reading of the manuscript. We thank CGC and Alexander M. van der Bliek for kindly sending us the *Pmyo-3::mito::GFP* constructs and worms. This work was supported by grants from the Chinese Ministry of Science and Technology (Grant #2011CB504206 and 2011CB809106), to J.D.J.H and Y.H., grants from the National Natural Science Foundation of China (Grant 31210103916, 91019019, 20890020, 90913011 and 21222501) to J.D.J.H and Y.H., and grants from Chinese Academy of Sciences (Grant #KSCX2-EW-R-02, KSCX2-EW-J-15, Y2201242 and XDA01010303) to J.D.J.H.

Author Contributions

JDJH conceived the project. YH, JDJH, JS, BX, and YP designed the fluidic device. JDJH, YH and BX, JS designed experiments. JDJH, WC, and NQ designed computational analyses. JS, BX, DJ, and YM implemented the fluidic device. BX, SJ, NS, and TY implemented the experiments. WC, NQ, and ZH implemented computational analysis. JDJH, BX, YH, JS, WC, NQ, and MK wrote the paper. JDJH and YH provided financial support.

References

Aitlhadj L, Sturzenbaum SR (2010) The use of FUdR can cause prolonged longevity in mutant nematodes. *Mech. Ageing Dev.* **131**, 364–365.

Bishop NA, Guarente L (2007) Two neurons mediate diet-restriction-induced longevity in *C. elegans*. *Nature* **447**, 545–549.

Brenner S (1974) The genetics of *Caenorhabditis elegans*. *Genetics* **77**, 71–94.

Davies SK, Leroi AM, Bundy JG (2012) Fluorodeoxyuridine affects the identification of metabolic responses to daf-2 status in *Caenorhabditis elegans*. *Mech. Ageing Dev.* **133**, 46–49.

Davis BO Jr, Anderson GL, Dusenbery DB (1982) Total luminescence spectroscopy of fluorescence changes during aging in *Caenorhabditis elegans*. *Biochemistry* **21**, 4089–4095.

Finkel T, Holbrook NJ (2000) Oxidants, oxidative stress and the biology of ageing. *Nature* **408**, 239–247.

Fraser AG, Kamath RS, Zipperlen P, Martinez-Campos M, Sohrmann M, Ahringer J (2000) Functional genomic analysis of *C. elegans* chromosome I by systematic RNA interference. *Nature* **408**, 325–330.

Gandhi S, Santelli J, Mitchell DH, Stiles JW, Sanadi DR (1980) A simple method for maintaining large, aging populations of *Caenorhabditis elegans*. *Mech. Ageing Dev.* **12**, 137–150.

Gerstbrein B, Stamatas G, Kollias N, Driscoll M (2005) In vivo spectrofluorimetry reveals endogenous biomarkers that report healthspan and dietary restriction in *Caenorhabditis elegans*. *Aging Cell* **4**, 127–137.

Greer EL, Maures TJ, Hauswirth AG, Green EM, Leeman DS, Maro GS, Han S, Banko MR, Gozani O, Brunet A (2010) Members of the H3K4 trimethylation complex regulate lifespan in a germline-dependent manner in *C. elegans*. *Nature* **466**, 383–387.

Huang C, Xiong C, Kornfeld K (2004) Measurements of age-related changes of physiological processes that predict lifespan of *Caenorhabditis elegans*. *Proc Natl Acad Sci U S A* **101**, 8084–8089.

Hulme SE, Shevkoplyas SS, McGuigan AP, Apfeld J, Fontana W, Whitesides GM (2010) Lifespan-on-a-chip: microfluidic chambers for performing lifelong observation of *C. elegans*. *Lab Chip* **10**, 589–597.

Joeng KS, Song EJ, Lee KJ, Lee J (2004) Long lifespan in worms with long telomeric DNA. *Nat. Genet.* **36**, 607–611.

Johnson TE (1990) Increased life-span of age-1 mutants in *Caenorhabditis elegans* and lower Gompertz rate of aging. *Science* **249**, 908–912.

Kenyon C (2005) The plasticity of aging: insights from long-lived mutants. *Cell* **120**, 449–460.

Kenyon CJ (2010) The genetics of ageing. *Nature* **464**, 504–512.

Klass MR (1977) Aging in the nematode *Caenorhabditis elegans*: major biological and environmental factors influencing life span. *Mech. Ageing Dev.* **6**, 413–429.

Labrousse AM, Zappaterra MD, Rube DA, van der Bliek AM (1999) *C. elegans* dynamin-related protein DRP-1 controls severing of the mitochondrial outer membrane. *Mol. Cell* **4**, 815–826.

Lee SS, Lee RY, Fraser AG, Kamath RS, Ahringer J, Ruvkun G (2003) A systematic RNAi screen identifies a critical role for mitochondria in *C. elegans* longevity. *Nat. Genet.* **33**, 40–48.

Lee SJ, Murphy CT, Kenyon C (2009) Glucose shortens the life span of *C. elegans* by downregulating DAF-16/FOXO activity and aquaporin gene expression. *Cell Metab.* **10**, 379–391.

Lee SS, Avalos Vizcarra I, Huberts DH, Lee LP, Heinemann M (2012) Whole lifespan microscopic observation of budding yeast aging through a microfluidic dissection platform. *Proc Natl Acad Sci U S A* **109**, 4916–4920.

Leiser SF, Begun A, Kaeberlein M (2011) HIF-1 modulates longevity and healthspan in a temperature-dependent manner. *Aging Cell* **10**, 318–326.

Lin K, Dorman JB, Rodan A, Kenyon C (1997) daf-16: an HNF-3/forkhead family member that can function to double the life-span of *Caenorhabditis elegans*. *Science* **278**, 1319–1322.

Martin GM, Austad SN, Johnson TE (1996) Genetic analysis of ageing: role of oxidative damage and environmental stresses. *Nat. Genet.* **13**, 25–34.

McCarroll SA, Murphy CT, Zou S, Pletcher SD, Chin CS, Jan YN, Kenyon C, Bargmann CI, Li H (2004) Comparing genomic expression patterns across species identifies shared transcriptional profile in aging. *Nat. Genet.* **36**, 197–204.

Mitchell DH, Stiles JW, Santelli J, Sanadi DR (1979) Synchronous growth and aging of *Caenorhabditis elegans* in the presence of fluorodeoxyuridine. *J Gerontol.* **34**, 28–36.

Morris JZ, Tissenbaum HA, Ruvkun G (1996) A phosphatidylinositol-3-OH kinase family member regulating longevity and diapause in *Caenorhabditis elegans*. *Nature* **382**, 536–539.

Ogg S, Paradis S, Gottlieb S, Patterson GI, Lee L, Tissenbaum HA, Ruvkun G (1997) The Fork head transcription factor DAF-16 transduces insulin-like metabolic and longevity signals in *C. elegans*. *Nature* **389**, 994–999.

Otsu N (1979). A threshold selection method from gray-level histograms. *IEEE Trans. Systems Man and Cybernet* **9**, 62–66.

Pincus Z, Slack FJ (2010) Developmental biomarkers of aging in *Caenorhabditis elegans*. *Dev. Dyn.* **239**, 1306–1314.

Pincus Z, Smith-Vikos T, Slack FJ (2011) MicroRNA predictors of longevity in *Caenorhabditis elegans*. *PLoS Genet.* **7**, e1002306.

Schlotterer A, Kukudov G, Bozorgmehr F, Hutter H, Du X, Oikonomou D, Ibrahim Y, Pfisterer F, Rabbani N, Thornalley P, Sayed A, Fleming T, Humpert P, Schwenger V, Zeier M, Hamann A, Stern D, Brownlee M, Bierhaus A, Nawroth P, Morcos M (2009) *C. elegans* as model for the study of high glucose- mediated life span reduction. *Diabetes* **58**, 2450–2456.

Schulz TJ, Zarse K, Voigt A, Urban N, Birringer M, Ristow M (2007) Glucose restriction extends *Caenorhabditis elegans* life span by inducing mitochondrial respiration and increasing oxidative stress. *Cell Metab.* **6**, 280–293.

Stephens GJ, Johnson-Kerner B, Bialek W, Ryu WS (2008) Dimensionality and dynamics in the behavior of *C. elegans*. *PLoS Comput. Biol.* **4**, e1000028.

Sutphin GL, Kaeberlein M (2009). Measuring *Caenorhabditis elegans* life span on solid media. *J. Vis Exp.* **27**, 1152.

Thorsen T, Maerkl SJ, Quake SR (2002) Microfluidic large-scale integration. *Science* **298**, 580–584.

Timmons L, Court DL, Fire A (2001) Ingestion of bacterially expressed dsRNAs can produce specific and potent genetic interference in *Caenorhabditis elegans*. *Gene* **263**, 103–112.

Unger MA, Chou HP, Thorsen T, Scherer A, Quake SR (2000) Monolithic microfabricated valves and pumps by multilayer soft lithography. *Science* **288**, 113–116.

Wahlby C, Kamentsky L, Liu ZH, Riklin-Raviv T, Conery AL, O'Rourke EJ, Sokolnicki KL, Visvikis O, Ljosa V, Irazoqui JE, Golland P, Ruvkun G, Ausubel FM, Carpenter AE (2012). An image analysis toolbox for high-throughput *C. elegans* assays. *Nat. Methods* **9**, 714–716.

Wang J, Zhou Y, Qiu H, Huang H, Sun C, Xi J, Huang Y (2009) A chip-to-chip nanoliter microfluidic dispenser. *Lab Chip* **9**, 1831–1835.

Xie Z, Zhang Y, Zou K, Brandman O, Luo C, Ouyang Q, Li H (2012). Molecular phenotyping of aging in single yeast cells using a novel microfluidic device. *Aging Cell* **11**, 599–606.

Xue H, Xian B, Dong D, Xia K, Zhu S, Zhang Z, Hou L, Zhang Q, Zhang Y, Han JD (2007) A modular network model of aging. *Mol Syst Biol.* **3**, 147.

Zahn JM, Poosala S, Owen AB, Ingram DK, Lustig A, Carter A, Weeraratna AT, Taub DD, Gorospe M, Mazan-Mamczarz K, Lakatta EG, Boheler KR, Xu X, Mattson MP, Falco G, Ko MS, Schlessinger D, Firman J, Kummerfeld SK, Wood WH 3rd, Zonderman AB, Kim SK, Becker KG (2007) AGEMAP: a gene expression database for aging in mice. *PLoS Genet.* **3**, e201.

Supporting Information

Additional Supporting Information may be found in the online version of this article at the publisher's web-site.

Fig. S1 The process of loading young adult worms into PDMS chamber.

Fig. S2 Worms living in PDMS chambers have a similar physiological growth as worms living on NGM plates.

Fig. S3 The reproducibility of worm lifespan assays upon RNAi of aging-related genes.

Fig. S4 The reproducibility of worm lifespan assays in glucose medium.

Fig. S5 Age-related changes in fluorescence intensities.

Fig. S6 Oxidative stress tolerance assay in WormFarm.

Fig. S7 Comparison of survival rates calculated from our computer program with or without considering clustered worms to those from manual counting.

Video S1 Load 2% pluronic solution to make the channel lubricant.

Video S2 Load young adult worms into PDMS chamber.

Video S3 Wash off the offspring of adult worms in PDMS chamber.

Video S4 Movie of 5-day old worms in PDMS chamber (upper panel, *sptf-3* RNAi; lower panel, Ctrl RNAi).

Video S5 Movie of 5-day old worms in PDMS chamber (upper panel, *age-1* RNAi; lower panel, *Y82E9BR.3* RNAi).

Note S1 Formulas for calculating worm features/phenotypes.

Note S2 WormFarm video analysis procedure.

Table S1 Log-rank test results between automatically counted mean lifespans of different repeats in RNAi experiments.

Table S2 Log-rank test results between automatically counted mean lifespans of different repeats of glucose die*t* test.

Table S3 Significances of difference between the RNAi groups for worm length, width, area and motility as determined by Student's *t*-test.

Table S4 Raw data for lifespan assays.

Table S5 Raw data for mitochondrial fluorescent density assay.

Table S6 Raw data of average values of worm phenotypic features used in principal component analysis.

Supplementary Materials

Fig. S1 The process of loading young adult worms into PDMS chamber.

(a) Load 2% pluronic solution to lubricate the channels. (b) and (c) Load worm suspension and adjust the total number of worms to ~40 per chamber. (d) Add bacteria solution (10^9 cells per mL).

Fig. S2 Worms living in PDMS chambers have a similar physiological growth as worms living on NGM plates.

(a) Photographs show that from adult day 2 to day8, the liquid cultured worms in PDMS chambers (upper panel) have a similar growth rate as those on NGM plates (lower panel), FUdR was used to inhibit the offspring growth on plates, and worms were transferred onto new plates on day 4 and day 8. (b) Quantitation of average size of worms from adult day 2 to day 8 in WormFarm (upper panel) , or on NGM plates (lower panel).

Fig. S3 The reproducibility of worm life span assays upon RNAi of aging-related genes.

(a) A replicate set of photographs of worms living in WormFarm under different RNAi conditions in a separate repeat. (b) Survival rate curves of worms in PDMS chambers upon different RNAi conditions when live worms were determined manually by watching movies (upper) or by computational program analyzing the movies (lower). (c) Comparison of the survival rates (manually counted) changing over time of two repeats in RNAi lifespan tests. Two repeats of the same experiment are shown in the same color of the curves.

Fig. S4 The reproducibility of worm life span assays in glucose medium.

(a) A replicate set of survival rate curves of worms in PDMS chambers fed different concentrations of glucose when live worms were determined manually by watching movies (upper panel) or by computational program analyzing the movies (middle panel), and the survival rate curves of worms under different concentrations of glucose on NGM plates when live worms were determined by conventional method (lower panel). (b) Scatter plots showing the repeatability of each group of two independent on-plate biological replicates. Survival rates of two different repeats against each other across the worm adult life span. The x- and y-axes indicate the survival rates of repeat 1 and repeat 2 on the indicated day of adult life, respectively. Pearson correlation coefficient ("Cor") between the repeats for all three groups is shown at the bottom of the panel. (c) Comparison of the survival rates (manually counted) changing over time of two repeats of lifespan under glucose treatment. Two repeats of the same experiment are shown in the same color of the curves.

Fig. S5 Age-related changes in fluorescense intensities.

(a) Photographs of fluorescent intensity of *Pmyo-3::mito::GFP* over age.

Fig. S6 Oxidative stress tolerance assay in WormFarm.

Survival rate of N2 worms under control, *daf-2* or *daf-16* RNAi starting from L1 and treated with paraquat (0.4M) on adult day 4.

Fig. S7. Comparison of survival rates calculated from our computer program with or without considering clustered worms to those from manual counting.
Shown in the figure are two batches of control experiment (glucose 0%) videos. Survival rates calculated from manual counting are more similar to those from our computer program considering clustered worms than those without considering clustered worms reflected by linear regression R^2 between two curves.

Table S1 Log-rank test results between automatically counted mean lifespans of different repeats in RNAi experiments

Table S2 Log-rank test results between automatically counted mean lifespans of different repeats of glucose diet test

Table S3 Significances of difference between the RNAi groups for worm length, width, area and motility as determined by Student's t-test

Table S4 Raw data for life span assays

Table S5 Raw data for mitochondrial fluorescent density assay

Table S6 Raw data of average values of worm phenotypic features used in principle component analysis

Video S1 Load 2% pluronic solution to make the channel lubricant

Video S2 Load young adult worms into PDMS chamber

Video S3 Wash off the offspring of adult worms in PDMS chamber

Video S4 Movie of 5-day old worms in PDMS chamber (upper panel, *sptf-3* RNAi; lower panel, Ctrl RNAi)

Video S5 Movie of 5-day old worms in PDMS chamber (upper panel, *age-1* RNAi; lower panel, *Y82E9BR.3* RNAi)

Note S1 Formulas for calculating worm features/phenotypes

1. Survival rate on day i $Sr_i = \frac{N_i}{N_1}$, where N_i is the worm number on day i.

$$A = \frac{\sum_{i=2,K,m;j=1,K,n_i} A_{i,j}}{\sum_{i=2,K,m} n_i}$$

2. Worm area , where m is the total number of frames, n_i is the number of live worms in frame i, $A_{i,j}$ is the area of the j-th single live worm in frame i.

$$C = \frac{\sum_{i=2,K,m;j=1,K,n_i} C_{i,j}}{\sum_{i=2,K,m} n_i}$$

3. Worm circumference , where m is the total number of frames, n_i is the number of live worms in frame i, $C_{i,j}$ is the circumference of the j-th single live worm in frame i.

$$W = \frac{\sum_{i=2,K,m;j=1,K,n_i} W_{i,j}}{\sum_{i=2,K,m} n_i} \qquad L = \frac{\sum_{i=2,K,m;j=1,K,n_i} L_{i,j}}{\sum_{i=2,K,m} n_i}$$

4. Worm width , worm length , where $W_{i,j} = \frac{C_{i,j} - \sqrt{C_{i,j}^{\ 2} - 16 \times \mathrm{A}_{i,j}}}{4}$, $L_{i,j} = \frac{C_{i,j} + \sqrt{C_{i,j}^{\ 2} - 16 \times \mathrm{A}_{i,j}}}{4}$, $C_{i,j}$ is the circumference of the j-th single live worm in frame i, $A_{i,j}$ is the area of the j-th single live worm in frame i, $W_{i,j}$ is the width of the j-th single live worm in frame i, $L_{i,j}$ is the length of the j-th single live worm in frame i. m is the total frame number, n_i is the live worm number in frame i.

$$Mo = \frac{\sum_{i=2,K,m;j=1,K,n_i} \frac{M_{i,j}}{A_{i,j}}}{k \times \sum_{i=2,K,m} n_i}$$

5. Worm mobility: , where m is the total number of frames, n_i is the number of live worms in frame i, $M_{i,j}$ is the moving area of the j-th single live worm in frame i, $A_{i,j}$ is the area of the j-th single live worm in frame i. k= 0.05 second per frame.

6. Pixel Intensity = (sum of gray scale values of all pixels of a worm) / (pixel counts of the worm).

7. Intensity variation = variance of gray scale values of all pixels of a worm.

8. Relative bright area= (pixels whose gray scale value <= 100) / (pixel counts in the worm).

9. $$Relative\ position = \begin{cases} \dfrac{BL - DE}{HBL}, & if\ (DE > HBL) \\ \dfrac{DE}{HBL}, & else \end{cases}$$, where BL is the backbone length measured in pixels; given x is the nearest backbone point of a pixel, DE is the distance from x to one end of the backbone. HBL is the half-length of backbone. This only measures the distribution against the midpoint of the worms without distinguishing heads from tails.

10. Bright spot distribution is represented by a vector of relative positions of the pixels with the top 10% gray scale values. The average value in a vector was used for PCA.

11. Average fluorescence intensity: $$F = \frac{\sum_{i=1,K,m;j=1,K,n_i} G_{i,j}}{\sum_{i=2,K,m} n_i}$$, where m is the total number of frames, n_i is the number objects in frame i, $G_{i,j}$ is the average grayscale intensity of the j-th objects in frame i.

Note S2 WormFarm video analysis procedure

1. Read the video file into MATLAB and split it into frames.

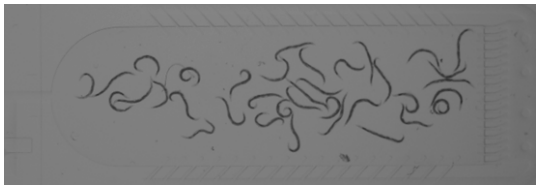

2. Recognize the chamber boundaries by using the relative distance from the circle to the boundaries (the relative distance from the circle to the boundaries are fixed). Each chamber is processed independently.

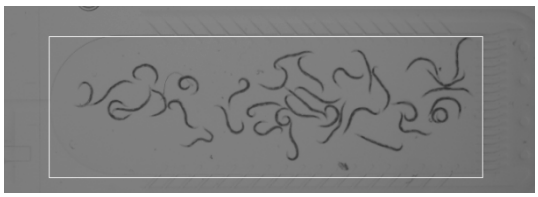

3. After the boundaries are found, the chamber regions are selected and converted from gray image to binary image using Otsu's method. The closed areas from the binary images are defined as worm-like objects (WLOs) and are filtered using the object area to remove small contaminants. Then compute the number of moving worms by detecting moving single worms and worm clusters with moving rate greater than the defined threshold, and compute single worms' moving area and motility (See Methods for formula and algorithm).

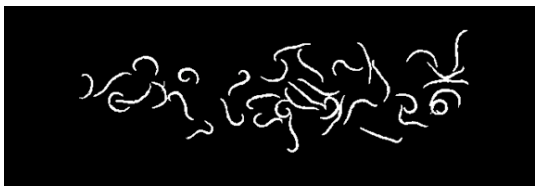

4. Detect single worms by size (See Methods for formula and algorithm). Then compute single worms' phenotypes, such as size, length, width, etc. The body area of each worm in binary image are recorded, and then mapped to the original gray images to compute the mean gray scale and variance of gray scales of each worm.

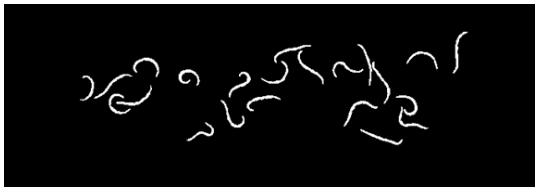

5. Extract each worm's backbone from the binary image, and compute the worm's shape and bright pixel distribution along the backbone.

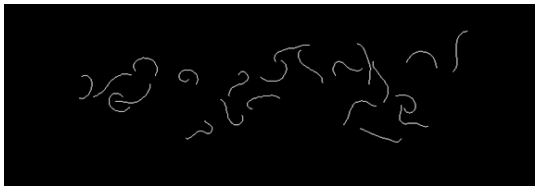

Fig. S1

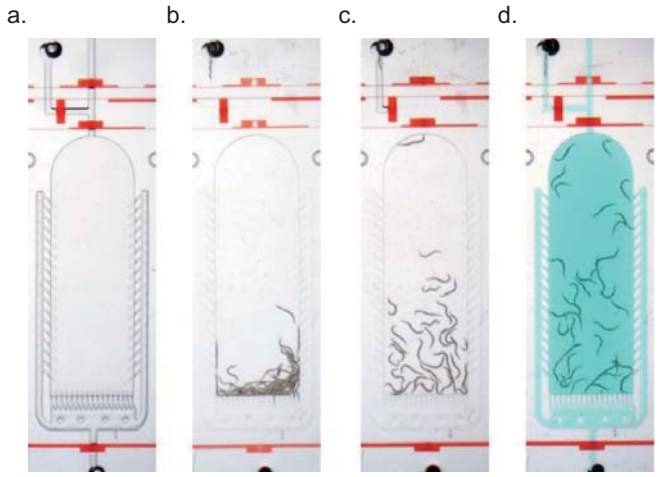
a.
b.
c.
d.

Fig. S2

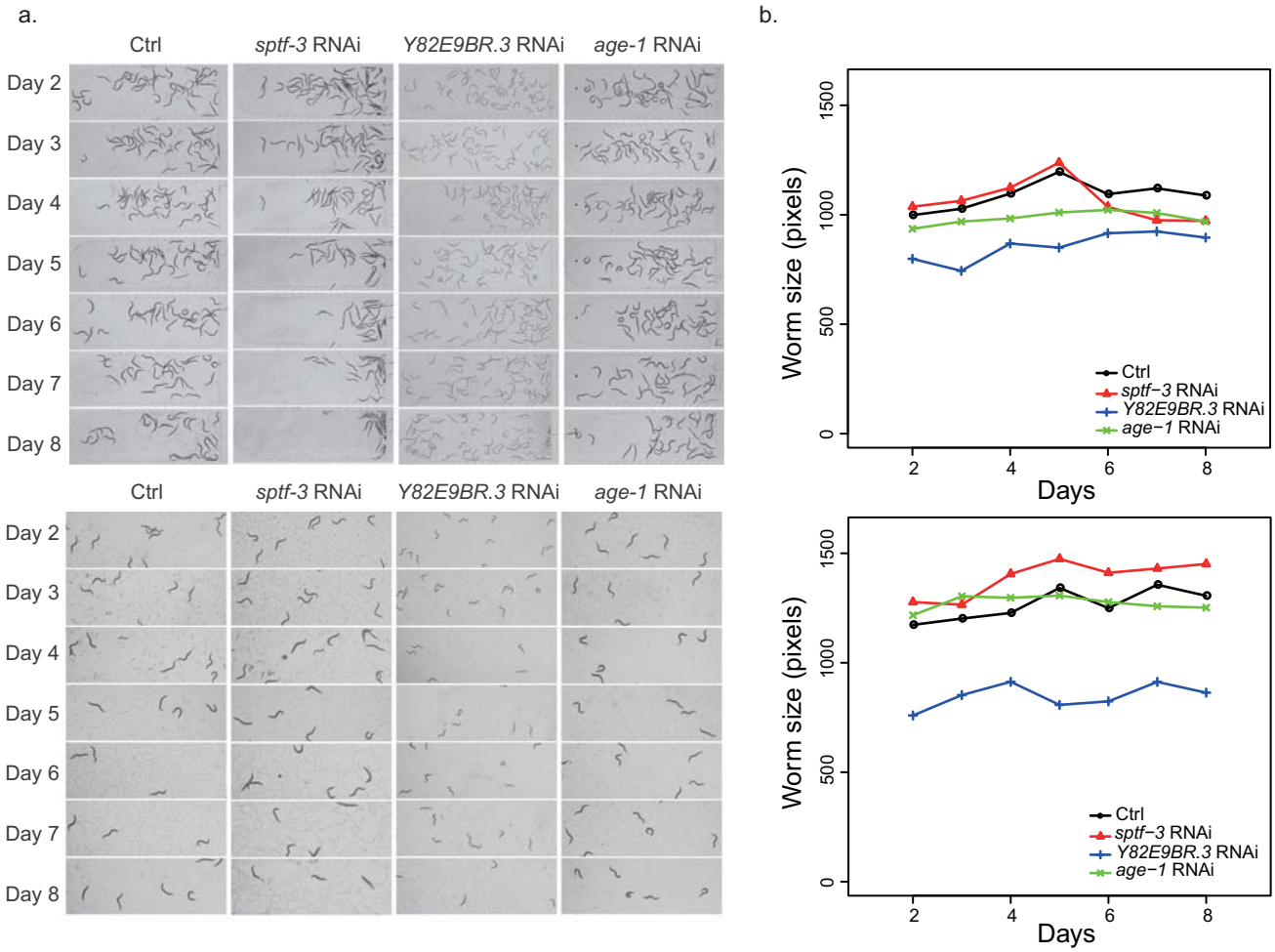
a.
Ctrl
sptf-3 RNAi
Y82E9BR.3 RNAi
age-1 RNAi
Day 2
Day 3
Day 4
Day 5
Day 6
Day 7
Day 8
b.
Worm size (pixels)
0
500
1000
1500
2
4
6
8
Days
Ctrl
sptf−3 RNAi
Y82E9BR.3 RNAi
age−1 RNAi

Fig. S3

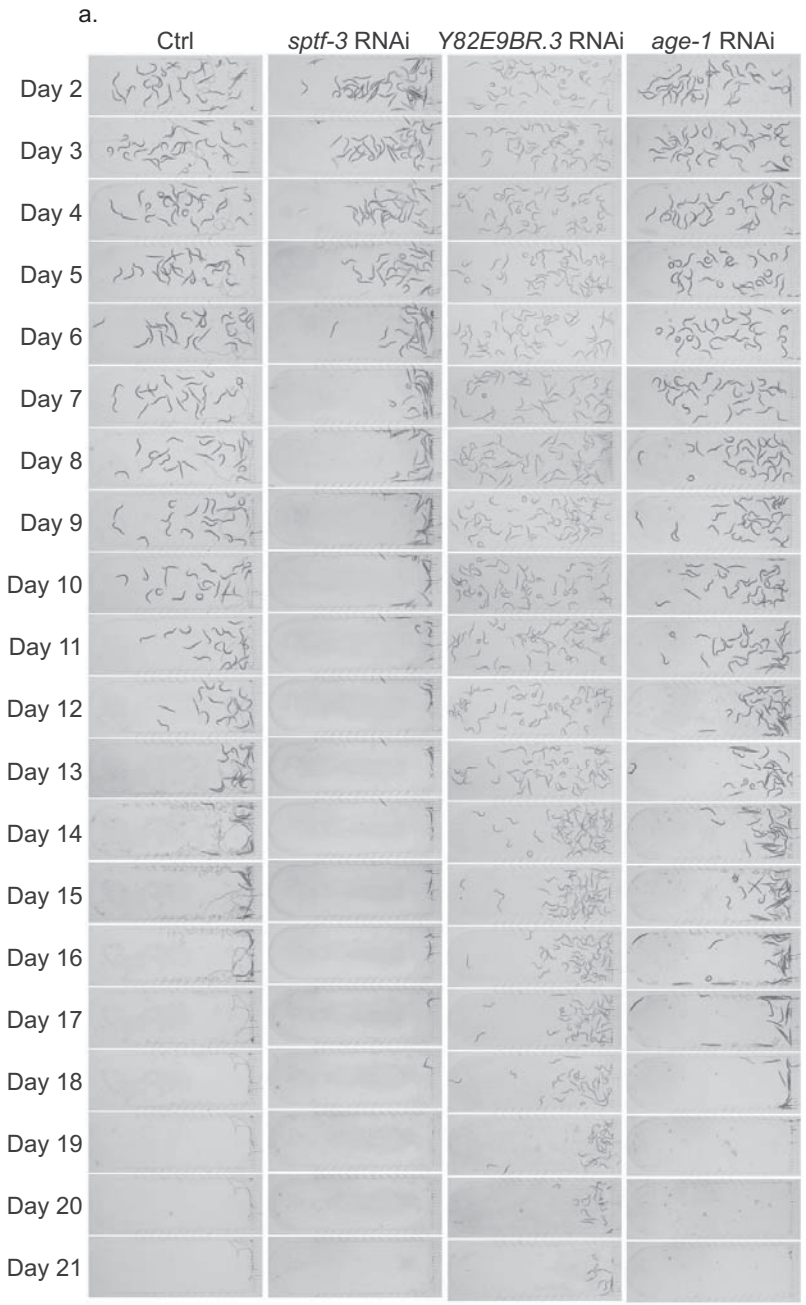
a.
Ctrl
sptf-3 RNAi
Y82E9BR.3 RNAi
age-1 RNAi
Day 2
Day 3
Day 4
Day 5
Day 6
Day 7
Day 8
Day 9
Day 10
Day 11
Day 12
Day 13
Day 14
Day 15
Day 16
Day 17
Day 18
Day 19
Day 20
Day 21

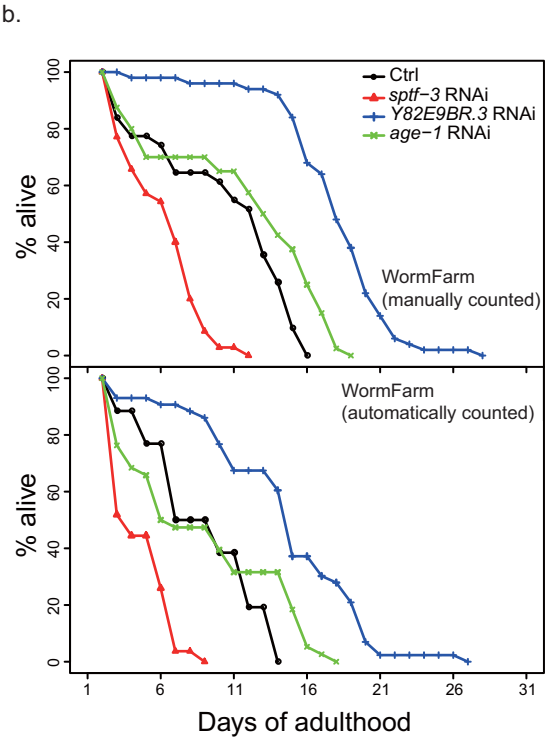
b.
Ctrl
sptf−3 RNAi
Y82E9BR.3 RNAi
age−1 RNAi
WormFarm
(manually counted)
WormFarm
(automatically counted)
% alive
Days of adulthood

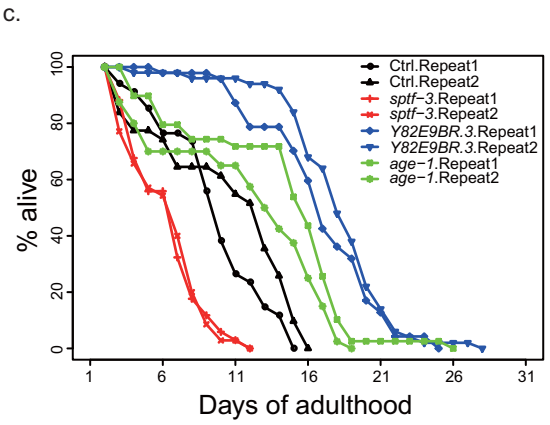
c.
Ctrl.Repeat1
Ctrl.Repeat2
sptf−3.Repeat1
sptf−3.Repeat2
Y82E9BR.3.Repeat1
Y82E9BR.3.Repeat2
age−1.Repeat1
age−1.Repeat2
% alive
Days of adulthood

Fig. S4

a.

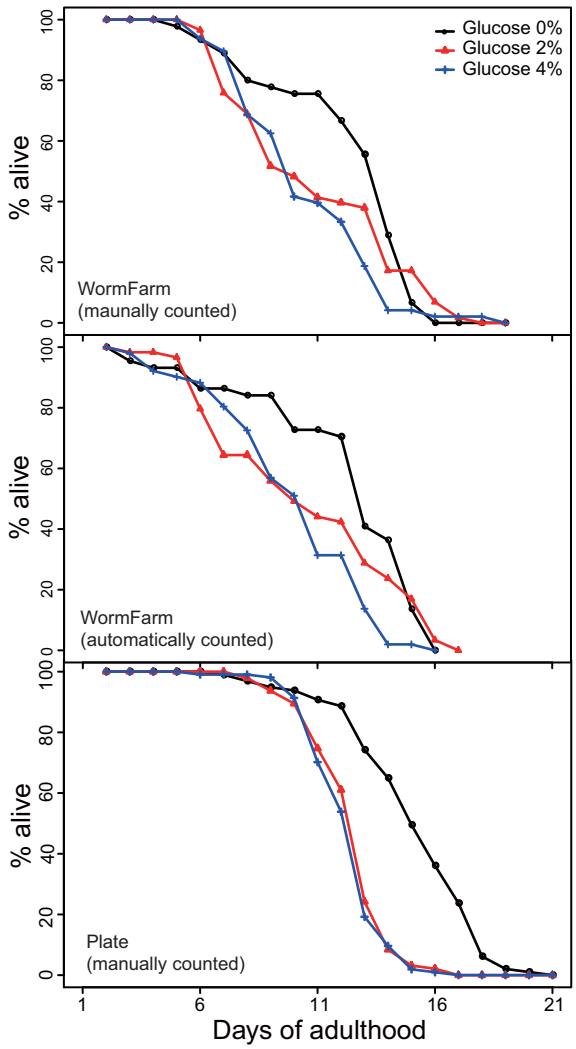
Glucose 0%
Glucose 2%
Glucose 4%
% alive
WormFarm
(maunally counted)
WormFarm
(automatically counted)
Plate
(manually counted)
Days of adulthood

b.

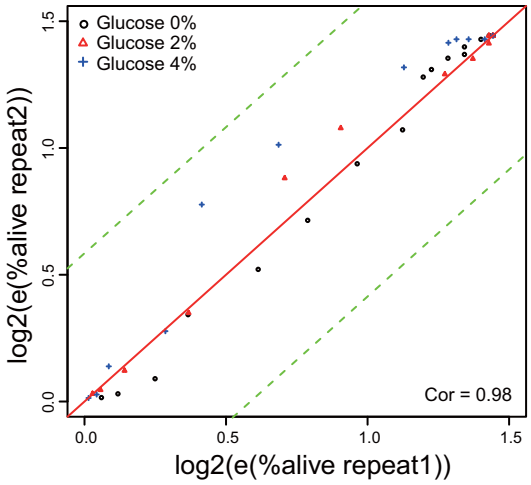
Glucose 0%
Glucose 2%
Glucose 4%
log2(e(%alive repeat2))
log2(e(%alive repeat1))
Cor = 0.98

c.

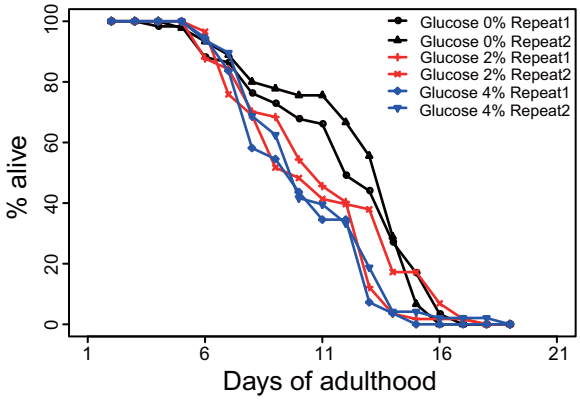
Glucose 0% Repeat1
Glucose 0% Repeat2
Glucose 2% Repeat1
Glucose 2% Repeat2
Glucose 4% Repeat1
Glucose 4% Repeat2
% alive
Days of adulthood

Fig. S5

a.

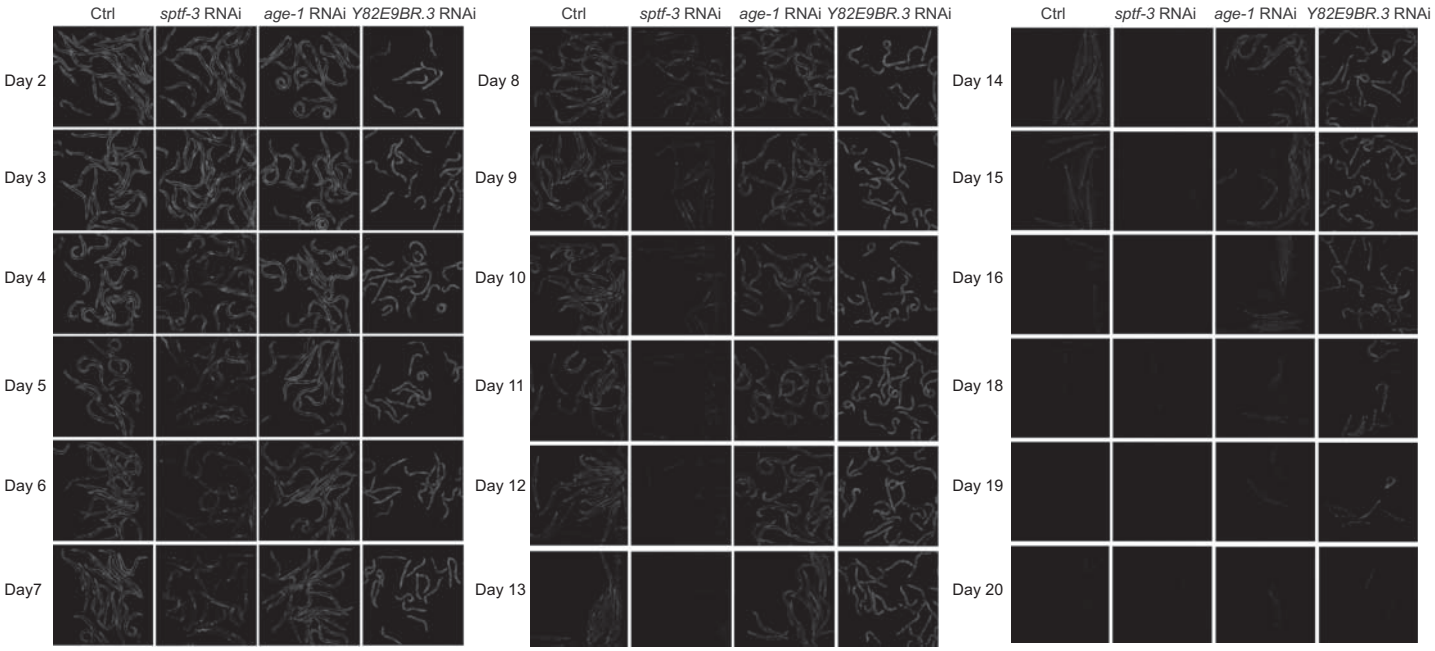
Ctrl
sptf-3 RNAi
age-1 RNAi
Y82E9BR.3 RNAi
Day 2
Day 3
Day 4
Day 5
Day 6
Day7
Day 8
Day 9
Day 10
Day 11
Day 12
Day 13
Day 14
Day 15
Day 16
Day 18
Day 19
Day 20

Fig. S6

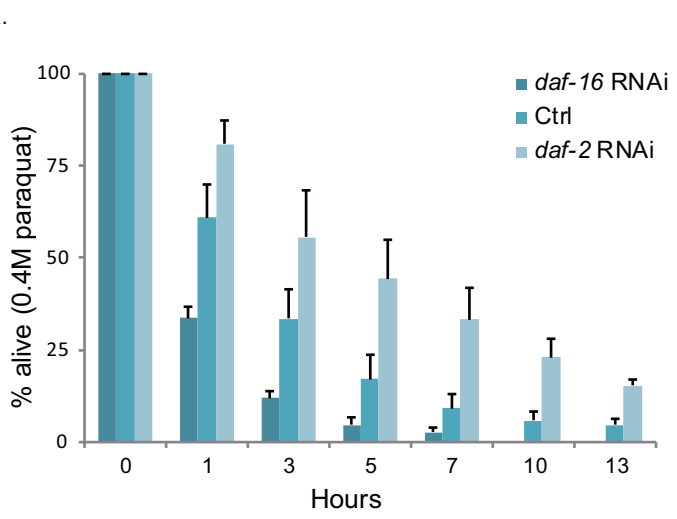
a.
100
75
50
25
0
% alive (0.4M paraquat)
daf-16 RNAi
Ctrl
daf-2 RNAi
0
1
3
5
7
10
13
Hours

Fig. S7

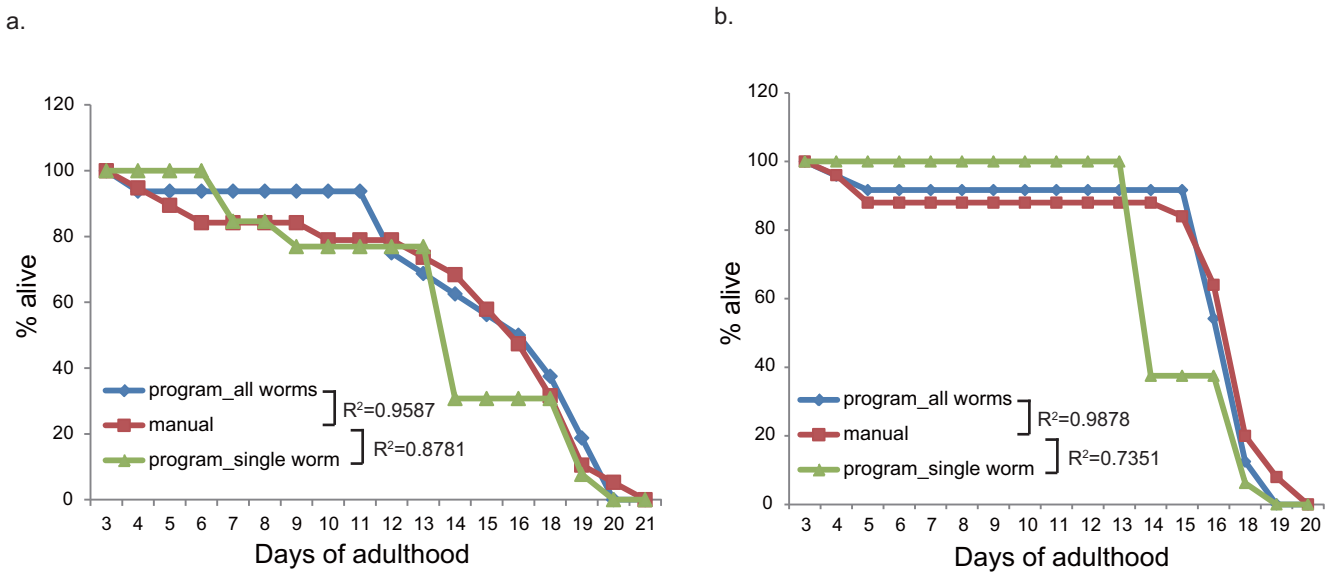
a.
120
100
80
60
40
20
0
% alive
program_all worms
manual
program_single worm
R²=0.9587
R²=0.8781
3 4 5 6 7 8 9 10 11 12 13 14 15 16 18 19 20 21
Days of adulthood
b.
120
100
80
60
40
20
0
% alive
program_all worms
manual
program_single worm
R²=0.9878
R²=0.7351
3 4 5 6 7 8 9 10 11 12 13 14 15 16 18 19 20
Days of adulthood

Table S1. Log-rank test results between automatically counted mean lifespans of different repeats in RNAi experiments

LogRank		*Ctrl*		*sptf-3 (RNAi)*		*age1 (RNAi)*		*Y82E9BR.3 (RNAi)*	
		R1	R2	R1	R2	R1	R2	R1	R2
Ctrl	R1	1	0.330997806	0.000686855	2.09795E-06	0.000126612	0.103288764	1.32971E-12	3.6945E-10
	R2	0.330997806	1	0.0000576	0.00000325	0.001659017	0.257654741	1.86E-09	1.96E-07
sptf-3 (RNAi)	R1	0.000686855	5.75507E-05	1	0.181810407	1.47782E-08	0.000321088	2.22045E-16	2.3204E-14
	R2	2.09795E-06	3.25048E-06	0.181810407	1	5.80297E-08	0.000164429	0	1.5543E-15
age1 (RNAi)	R1	0.000126612	0.001659017	1.48E-08	0.000000058	1	0.014509024	0.024275921	0.03755128
	R2	0.103288764	0.257654741	0.000321088	0.000164429	0.014509024	1	0.00000608	0.0000224
Y82E9BR.3 (RNAi)	R1	1.33E-12	1.86E-09	2.22E-16	0	0.024275921	0.00000608	1	0.87467149
	R2	3.69E-10	0.000000196	2.32E-14	1.55E-15	0.037551276	0.0000224	0.874671491	1

Color Code: Red: P=<0.01, Orange: 0.01<P<=0.05, Yellow 0.05<P<=0.1, Light Green 0.1<P<=0.15, Dark Green P>0.15

Table S2. Log-rank test results between automatically counted mean lifespans of different repeats of glucose diet test

LogRank		Ctrl		glucose 2%		glucose 4%	
		R1	R2	R1	R2	R1	R2
Ctrl	R1	1	0.989802281	0.000912014	0.223855934	0.000436467	0.000203658
	R2	0.989802281	1	0.000140489	0.240599645	0.0000608	0.00003
glucose 2%	R1	0.000912014	0.000140489	1	0.136878036	0.846990156	0.70594211
	R2	0.223855934	0.240599645	0.136878036	1	0.064358885	0.070374616
glucose 4%	R1	0.000436467	0.0000608	0.846990156	0.064358885	1	0.944814516
	R2	0.000203658	0.00003	0.70594211	0.070374616	0.944814516	1

Color Code: Red: P=<0.01, Orange: 0.01<P<=0.05, Yellow 0.05<P<=0.1, Light Green 0.1<P<=0.15, Dark Green P>0.15

Table S3. Significances of differences between the RNAi groups for worm length, width, area and motility as determined by Student's t-test

Phenotype	RNAi	Mean	STD	Difference from co	P-Value
Size	**ctrl**	233.47	14.39		
	sptf-3	218.88	12.78	-6.25%	1.89E-05
	age1	217.20	7.45	-6.97%	2.68E-07
	Y82E9BR.3	181.27	15.55	-22.36%	< 2.2e-16
Length	**ctrl**	50.53	2.86		
	sptf-3	45.51	3.50	-9.93%	2.56E-06
	age1	50.26	2.17	-0.53%	7.14E-01
	Y82E9BR.3	46.98	3.68	-7.03%	2.29E-06
Width	**ctrl**	4.69	0.16		
	sptf-3	4.94	0.44	5.33%	4.84E-02
	age1	4.33	0.14	-7.68%	3.39E-12
	Y82E9BR.3	3.86	0.24	-17.70%	< 2.2e-16
Mobility	**ctrl**	1.49	1.13		
	sptf-3	0.90	0.86	-39.60%	3.35E-05
	age1	2.46	0.82	65.10%	1.75E-06
	Y82E9BR.3	3.71	2.16	148.99%	3.43E-09

Table S4. Raw data for lifespan assays

RNAi lifespan raw data

Group	RNAi	Number of worms
WormFarm manually counted (repeat1, begin from day2, oneday interval)	ctrl	34,32,31,29,26,26,25,19,13,9,8,5,4,0
	sptf-3	34,30,23,19,19,11,6,4,2,1,0
	age1	39,39,35,35,31,31,29,29,29,28,28,28,28,21,17,10,4,1,1,1,1,1,1,1,0
	Y82E9BR.3	47,47,47,47,46,46,46,46,45,41,37,37,37,33,28,20,17,15,8,6,2,2,2,0
WormFarm automatically counted (repeat1, begin from day2, oneday interval)	ctrl	32,31,31,27,22,17,10,10,7,7,7,2,0
	sptf-3	32,17,17,12,10,7,6,6,0
	age1	35,30,30,30,23,23,23,23,23,17,17,17,17,14,6,4,2,1,1,0
	Y82E9BR.3	44,44,44,44,41,41,36,36,36,36,36,36,24,16,16,15,9,7,4,1,1,1,1,0
WormFarm manually counted (repeat2, begin from day2, oneday interval)	ctrl	31,26,24,24,23,20,20,20,19,17,16,11,8,3,0
	sptf-3	35,27,23,20,19,14,7,3,1,1,0,0,0,0,0
	age1	40,35,32,28,28,28,28,28,26,26,23,20,17,15,10,6,1,0,0,0,0
	Y82E9BR.3	50,50,49,49,49,49,48,48,48,48,47,47,46,42,34,32,24,19,11,7,3,2,1,1,1,1,0
WormFarm automatically counted (repeat2, begin from day2, oneday interval)	ctrl	26,23,23,20,20,13,13,13,10,10,5,5,0
	sptf-3	27,14,12,12,7,1,1,0
	age1	38,29,26,25,19,18,18,18,15,12,12,12,12,7,2,1,0
	Y82E9BR.3	43,40,40,40,39,39,38,37,33,29,29,29,26,16,16,13,12,9,3,1,1,1,1,1,1,0
NGM plate (begin from day2, oneday interval)	ctrl	59,59,59,59,59,58,57,47,40,33,13,8,4,2,1,0
	sptf-3	60,60,53,50,47,33,17,6,3,0
	age1	53,53,53,53,53,53,53,53,51,47,41,39,37,30,25,18,12,11,8,5,3,2,1,0
	Y82E9BR.3	75,75,75,75,75,75,75,75,74,73,72,64,62,57,52,46,37,29,25,16,5,2,2,1,1,0

Glucose lifespan raw data

Group	Growth condi	Number of worms
WormFarm manually counted (repeat1, begin from day2, oneday interval)	ctrl	59,59,58,58,52,51,45,43,40,39,29,26,16,10,2,0
	glucose 2%	57,57,57,57,50,48,40,39,31,26,23,7,2,1,1,1,0
	glucose 4%	55,55,55,55,52,46,32,30,24,19,19,4,2,0
WormFarm automatically counted (repeat1, begin from day2, oneday interval)	ctrl	61,61,58,57,51,50,47,44,44,32,31,27,20,11,3,0
	glucose 2%	57,57,53,50,45,43,34,34,34,27,25,4,1,1,1,0
	glucose 4%	53,53,52,50,44,39,28,28,28,23,20,4,4,0
WormFarm manually counted (repeat2, begin from day2, oneday interval	ctrl	45,45,45,44,42,40,36,35,34,34,30,25,13,3,0
	glucose 2%	58,58,58,58,56,44,40,30,28,24,23,22,10,10,4,1,0

from day2, oneday interval)	glucose 4%	48,48,48,48,45,43,33,30,20,19,16,9,2,2,1,1,1,0
WormFarm automatically counted (repeat2, begin from day2, oneday interval)	ctrl	44,42,41,41,38,38,37,37,32,32,31,18,16,6,0
	glucose 2%	59,58,58,57,47,38,38,33,29,26,25,17,14,10,2,0
	glucose 4%	51,50,47,46,45,41,37,29,26,16,16,7,1,1,0
NGM plate (repeat1, begin from day2, oneday interval)	ctrl	99,99,99,99,98,96,92,92,88,84,82,77,66,54,42,25,17,8,4,2,0
	glucose 2%	102,102,102,102,102,101,101,97,90,64,50,26,10,4,2,2,0
	glucose 4%	101,101,101,101,99,95,92,90,79,48,29,20,6,3,1,1,1,0
NGM plate (repeat2, begin from day2, oneday interval)	ctrl	97,97,97,97,97,96,94,92,91,88,86,72,63,48,35,23,6,2,1,0
	glucose 2%	95,95,95,95,95,95,93,89,85,71,58,23,8,3,2,0
	glucose 4%	104,104,104,104,103,103,103,102,95,73,56,20,10,2,1,0

Table S5. Raw data for mitochondrial fluorescent density assay

Ctrl					
Age/Day	Mean mitochondrial fluorescent density			Average	Standard deviation
	Chamber 1	Chamber 2	Chamber 3		
2	29.13908	28.36636	29.22605	28.9105	0.473239
3	27.55652	25.84734	22.77491	25.39292	2.422976
4	23.66006	23.25358	22.19358	23.03574	0.757119
5	19.28955	21.06793	20.73057	20.36268	0.944546
6	17.39673	18.56281	18.78847	18.24934	0.746949
7	14.29611	15.99535	16.04381	15.44509	0.995341
8	15.61945	14.02538	16.24251	15.29578	1.143452
9	15.2961	14.27673	14.70716	14.76	0.511734
10	14.19565	14.16747	14.18939	14.18417	0.014797
11	12.62537	13.38684	14.35278	13.45499	0.865716
12	12.78449	12.70598	12.37036	12.62028	0.219968
13	13.07682	12.38978	12.65709	12.70789	0.346328
14	12.25661	12.12056	12.281	12.21939	0.086457
15	12.26975	12.21565	11.54391	12.00977	0.40435
16	11.33815	10.72486	10.25999	10.77433	0.540781
17	10.6328	10.4778	9.721592	10.2774	0.487541
18	9.811946	9.843954	9.572664	9.742855	0.148256
19	9.418502	9.11708	9.862426	9.466003	0.374937
20	7.774014	9.354061	9.533798	8.887291	0.968306
21	7.526252	8.303304	10.1094	8.646318	1.325294
22	5.41501	8.159213	9.057008	7.543744	1.897403

***sptf-3* RNAi**					
Age/Day	Mean mitochondrial fluorescent intensity			Average	Standard deviation
	Chamber 1	Chamber 2	Chamber 3		
2	28.81124	28.41041	30.63666	29.2861	1.186663
3	25.73682	23.44127	24.16533	24.4478	1.173557
4	20.67418	20.25519	17.71064	19.54667	1.60379
5	16.50987	17.5032	17.71759	17.24355	0.644367
6	14.33481	15.03179	14.30396	14.55685	0.411598
7	12.10132	13.52756	14.16299	13.26396	1.055808
8	11.47305	11.5131	11.40649	11.46421	0.05385
9	10.48084	10.88251	10.51959	10.62765	0.221562
10	11.043	10.6233	10.0731	10.5798	0.486411
11	10.46731	11.03857	9.658974	10.38829	0.693187
12	9.553348	10.85911	8.991444	9.801299	0.958201
13	9.49085	10.08368	9.025235	9.533256	0.530497
14	8.928008	10.00915	8.566992	9.168049	0.750445
15	8.071759	9.587401	7.250012	8.303057	1.185736
16	6.479422	9.023995	6.157738	7.220385	1.570231

***Y82E9BR.3* RNAi**					
Age/Day	Mean mitochondrial fluorescent intensity			Average	Standard deviation
	Chamber 1	Chamber 2	Chamber 3		
2	38.96698	40.12429	41.29139	40.12756	1.162205
3	35.01148	36.92977	36.46268	36.13464	1.000331
4	31.38064	32.58306	32.50701	32.1569	0.673337
5	28.06169	28.49633	28.59486	28.38429	0.283691
6	26.08748	28.46651	27.33782	27.29727	1.190033
7	22.92402	25.95746	24.35265	24.41138	1.517571
8	19.75316	22.44839	22.20439	21.46864	1.490658
9	20.37401	20.93467	21.10145	20.80338	0.381074
10	17.86343	20.41414	20.49287	19.59015	1.495902
11	17.98525	20.38214	19.203	19.19013	1.198497
12	18.30933	18.7885	20.48725	19.19503	1.144456
13	17.35427	17.43692	18.76283	17.85134	0.790453
14	17.64682	17.67352	18.56434	17.96156	0.522194
15	15.6831	16.33547	19.5154	17.17799	2.05037
16	16.38603	16.42848	18.53159	17.11537	1.226666
17	15.05644	14.22157	15.32805	14.86869	0.576637
18	13.65879	14.09311	16.6667	14.8062	1.625808
19	18.24242	13.47554	14.28594	15.33463	2.550608
20	15.23445	11.29988	13.2927	13.27568	1.967341
21	13.05775	12.8577	11.22604	12.3805	1.004776
22	13.62078	13.07432	9.82409	12.17306	2.052539
23	11.3197	11.38927	8.631773	10.44692	1.572345
24	10.76774	11.69934	12.05885	11.50864	0.66634
25	9.815389	11.49062	9.809364	10.37179	0.968937

age-1 RNAi					
Age/Day	Mean mitochondrial fluorescent intensity			Average	Standard deviation
	Chamber 1	Chamber 2	Chamber 3		
2	30.04232	26.46638	30.37317	28.96062	2.166403
3	27.70538	25.31753	28.29684	27.10658	1.577336
4	24.92471	22.31836	24.23621	23.82642	1.350633
5	20.11232	19.5576	23.1705	20.94681	1.945642
6	17.51733	17.051	19.33965	17.96933	1.209424
7	14.57329	14.88883	17.66154	15.70789	1.699255
8	14.72734	13.96824	15.93742	14.87767	0.99316
9	14.46265	13.26182	15.11406	14.27951	0.9396
10	13.54873	12.64405	14.15728	13.45002	0.761428
11	13.62051	12.03882	13.52977	13.06303	0.888153
12	12.31903	10.92056	12.73782	11.99247	0.951622
13	13.30142	10.75046	12.36867	12.14018	1.290739
14	12.03245	11.20472	12.53293	11.92337	0.670792
15	11.85303	11.34156	12.73528	11.97663	0.705031
16	11.16312	11.2864	12.13575	11.52842	0.529562
17	9.602254	10.50923	11.05054	10.38734	0.731798
18	9.998276	10.37075	12.4332	10.93407	1.311572
19	9.382028	10.92598	10.75075	10.35292	0.845369
20	9.178672	9.622982	10.2847	9.69545	0.556562
21	8.456756	9.916194	10.11225	9.495067	0.904531
22	9.077446	9.645966	10.4577	9.727037	0.693688
23	8.843704	8.667155	9.382145	8.964335	0.372447
24	8.580127	9.80409	9.81135	9.398522	0.70876

Table S6. Raw data of average values of worm phenotypic features used in principle component analysis

Group	Date	Average shape	Average size	Average width	Average length	Average gray values	Average variance of gray values	Average ratio of pixels deep than threshold	Average brighter pixels distribution
Ctrl	20110725	0.646627	164.896552	3.242227	50.859895	87.247399	108.181589	0.869233	0.663089
	20110726	0.607958	162.744	3.393015	48.054985	85.740925	107.385484	0.929134	0.630844
	20110727	0.620188	166.190341	3.39565	48.973668	85.977859	104.93391	0.922943	0.65062
	20110728	0.731061	177.667925	3.522907	50.394074	88.697845	109.774375	0.837624	0.653417
	20110729	0.525262	169.957746	3.537141	48.223423	91.233037	77.633117	0.760056	0.672774
	20110730	0.48054	157.304348	3.278631	47.833687	90.164804	57.566259	0.883581	0.651286
	20110731	0.559399	180.482234	3.55711	50.41751	91.989945	64.514372	0.80213	0.603594
	20110801	0.493103	173.512	3.589673	48.658327	91.749065	60.990775	0.795438	0.6022
	20110802	0.400775	201.233577	3.679601	54.842297	93.821332	63.98849	0.747113	0.570515
	20110803	0.843997	200.544554	3.805305	52.689744	88.939429	54.792622	0.931566	0.51964
	20110804	0.703226	177.5625	3.665913	48.496587	89.751862	45.357514	0.953214	0.558024
	20110805	0.397797	167.53211	3.497066	47.677246	87.013251	47.652284	0.999846	0.513867
	20110806	0.458818	160.011765	3.238979	49.055139	85.407088	47.245418	1	0.441315
	20110807	0.740962	192.808511	3.728117	51.463372	83.432807	52.927531	1	0.465639
	20110808	0.269746	214.289474	3.492782	61.67827	85.057856	53.280703	0.999885	0.386196
	20110809	0.305985	162.578947	3.224098	50.802218	82.481451	46.926359	1	0.564169
	20110810	0.298448	179.825	3.576007	50.605243	84.721001	79.507175	0.956058	0.667045
	20110811	0.243024	177.052632	3.5936	49.301137	79.314939	85.337002	1	0.599205
	20110816	0.505216	199	3.523595	56.476405	88.678392	19.390995	1	0.735802
sptf-3 (RNAi)	20110725	0.465856	188.504249	3.647843	51.900316	86.715889	88.114004	0.922605	0.638574
	20110726	0.552086	177.985222	3.509481	50.752835	87.96671	93.321873	0.878366	0.642327
	20110727	0.453788	180.780549	3.674093	49.223662	88.037742	91.725451	0.861027	0.585273
	20110728	0.5525	177.895349	3.740984	47.587504	89.830481	96.706074	0.830087	0.5496
	20110729	0.392305	161.681034	3.494945	46.246434	87.288593	78.44884	0.919922	0.575838
	20110730	0.46164	173.187097	3.838745	45.093513	87.863886	48.551359	0.925744	0.501748
	20110731	0.302762	160.982143	3.544411	45.366304	85.430215	52.926456	1	0.589764
	20110801	0.236067	158.630435	3.509736	45.109829	86.858419	75.947767	0.873089	0.634865
	20110802	0.476449	165.863309	3.69669	44.767339	86.92322	62.815196	1	0.634165
	20110803	0.36742	158.961538	3.285495	47.618351	85.849843	58.003208	0.962436	0.558849
	20110804	0.364394	186.191489	4.054229	45.956409	89.770836	57.741071	0.877199	0.652418
	20110805	0.217382	197.928571	3.774207	52.511507	84.800792	99.751036	0.975922	0.728088
	20110806	0.253842	183.923077	3.672044	50.135648	83.055928	96.155669	1	0.728803
	20110807	0.19716	190.808511	3.546014	53.496539	87.931115	89.036089	0.897094	0.637807
	20110813	0.208925	217	5.262157	41.237843	96.036866	31.369005	0.718894	0.843478
	20110815	0.192275	178.05	3.108183	57.316817	96.097887	60.499273	0.669429	0.739524
age-1 (RNAi)	20110725	0.704062	172.066667	3.401257	50.619854	79.903249	128.730868	0.971399	0.579962
	20110726	0.659203	159.508889	3.358202	47.506242	77.982459	116.255802	1	0.575803
	20110727	0.486913	167.313433	3.461268	48.206642	76.840312	111.429984	0.992668	0.606686
	20110728	0.640035	172.569733	3.368199	51.069486	79.459093	116.481917	0.974057	0.587802
	20110729	0.593532	191.890805	3.53299	54.523045	82.547036	108.550835	0.9382	0.576702
	20110730	0.53294	187.333333	3.595673	51.967923	82.454161	107.065158	0.979273	0.524282
	20110731	0.554914	181.892241	3.521361	51.457088	83.875551	89.361002	0.955679	0.581369
	20110801	0.531448	193.060109	3.658468	52.77869	87.961034	95.700554	0.863629	0.498801
	20110802	0.506993	194.729323	3.815533	51.10364	85.688772	98.832576	0.924682	0.522308
	20110803	0.587543	186.742857	3.65183	51.34817	86.419004	81.649177	0.940957	0.549399
	20110804	0.473668	185.953216	3.467105	53.573831	86.106181	72.106602	0.95701	0.477916
	20110805	0.536115	189.930818	3.651865	51.901594	86.456133	75.064142	0.928032	0.513666
	20110806	0.619458	183.439153	3.539999	51.843599	81.37544	87.40119	0.993662	0.55661
	20110807	0.516525	186.239726	3.659171	51.022336	79.056905	94.466192	1	0.510596

	20110808	0.591861	141.959184	3.166779	45.40465	79.959354	84.13596	0.999491	0.568683
	20110809	0.321616	189.482143	3.347121	56.617164	75.492651	87.958384	1	0.5005
	20110810	0.357426	167.618182	3.729972	45.129119	77.732612	78.189807	1	0.491441
	20110811	0.390202	177.619048	3.446339	51.506042	77.022859	86.891354	1	0.611591
	20110812	0.227455	187.326531	3.532852	53.497761	76.739898	72.024266	1	0.521548
	20110813	0.178079	211.85	3.637213	58.262787	75.308687	98.972383	1	0.697778
	20110815	0.258255	146.660714	3.239786	45.010214	92.705935	63.436174	0.88629	0.546707
	20110816	0.392273	113	3.104805	36.395195	91.654867	20.69232	1	0.507177
Y82E9BR.3 (RNAi)	20110725	0.658294	89.214876	2.8086	31.72859	102.601925	31.689767	0.366616	0.612102
	20110726	0.557658	96.769231	2.740844	35.317329	103.938896	37.330683	0.290785	0.607791
	20110727	0.666825	98.597625	2.801095	35.212098	102.71194	35.952103	0.345637	0.625369
	20110728	0.68542	101.361702	2.740602	36.846499	104.732926	37.20161	0.238385	0.632221
	20110729	0.699184	104.231441	2.877679	36.192736	103.804662	35.039253	0.302099	0.620864
	20110730	0.609579	105.538622	3.071989	34.496905	106.028629	30.24922	0.17738	0.604496
	20110731	0.648888	106.199498	2.846875	37.169436	105.171641	31.101803	0.209672	0.606991
	20110801	0.640175	105.454545	2.933305	36.049212	104.552396	30.162979	0.247437	0.613837
	20110802	0.535395	113.337727	3.056742	36.816405	104.430111	32.24796	0.249664	0.589868
	20110803	0.779989	116.884712	3.085282	37.845796	103.485046	33.325442	0.30411	0.608924
	20110804	0.662379	109.805369	2.993547	36.484082	102.875348	32.613275	0.333511	0.604685
	20110805	0.727096	106.219672	2.873503	36.754366	99.741249	34.681932	0.501066	0.623339
	20110806	0.752494	113.787879	2.961323	38.187162	101.145863	38.045158	0.425184	0.573682
	20110807	0.60075	115.122807	3.019029	38.273368	101.649922	32.552797	0.413631	0.576733
	20110808	0.649916	113.235474	3.024409	37.327273	97.31763	48.430603	0.610187	0.572065
	20110809	0.681379	105.296443	2.765589	37.819392	96.697533	41.13512	0.678255	0.57168
	20110810	0.465633	111.93578	2.910316	38.484179	92.198325	52.380088	0.850133	0.550326
	20110811	0.332512	119.874214	3.105682	38.523249	94.340641	47.438704	0.761854	0.540615
	20110812	0.513526	118.646018	3.005073	39.499352	94.459532	40.458534	0.805658	0.552979
	20110813	0.290737	113.264901	3.020939	37.439326	90.520945	48.282849	0.880845	0.630953
	20110814	0.843639	121.35	3.060927	39.714073	98.729488	71.030053	0.576508	0.507965
	20110815	0.292607	113.7	3.804182	29.895818	104.115286	39.368162	0.343072	0.462623
	20110816	0.257654	124.333333	2.787929	44.065013	85.878146	75.290745	1	0.63102